Available online at www.sciencedirect.com
SCIENCE DIRECT
Catalysis Today 105 (2005) 254–274
CATALYSIS TODAY
www.elsevier.com/locate/cattod

Spatiotemporal patterns in catalytic systems

Dan Luss [a,*], Moshe Sheintuch [b,1]

[a] Department of Chemical Engineering, University of Houston, Houston, TX 77204-4004, USA
[b] Department of Chemical Engineering, Technion, Haifa 32000, Israel

Abstract

Infrared thermography measurements in various oxidation reactions revealed high-temperature domains whose boundaries are either stationary, oscillating, moving or rotating. These motions were observed on catalytic wires, rings, cylindrical pellets and thin catalytic beds. Their evolutions are different from the classical Turing mechanism, which explains many of the pattern formation in reaction–diffusion system. The observed patterns are strongly affected by the interaction between the local surface reaction rate, the mixing in the surrounding reactant phase and by the intrinsic heterogeneity of the catalytic surface and the transport coefficients. While simulations can qualitatively predict such patterns, quantitative predictions require a reliable kinetic model. Formation of hot regions in a three-dimensional fixed-bed can be predicted with reliable kinetic models. While formation of hot regions in the flow direction in the reactor are reasonably well understood, there is still a need to gain qualitative understanding as well as design criteria for formation of hot zones transversal to the flow direction.

Keywords: Catalytic systems; Hot zones; Spatiotemporal patterns; Global coupling; Impact of non-uniformities

1. Introduction

For many years, it was assumed that the state of catalytic surfaces is stationary (in time) and symmetric (in space). While the temporal dynamics of such models have been extensively studied in the past 40 years, the observations and analysis of spatial symmetry breaking have emerged mainly in the past two decades. The transversal temperature profile in a packed-bed reactor, for example, is usually assumed to be symmetric. It is either uniform (in an adiabatic reactor) or just a function of the radial position (in a cooled reactor). However, industrial experience has indicated that in certain cases this symmetry breaks up and local hot zones form in the reactor. These hot zones obviously affect the conversion of the reactants and the yield of the desired product. They may also pose severe safety problems by damaging the reactor structure. For example, clinkers of fused catalysts are often found during the replacement of the catalyst in trickle-bed reactors used to hydrogenate hydrocarbons, indicating that local hot zones existed in the reactor. A hot zone present next to the reactor wall can decrease its strength and lead to a leak of the reactants and a subsequent explosion. Barkelew and Gambhir [1] presented guidelines for preventing the formation of such hot spots. The understanding and ability to predict the conditions leading to evolution of local hot zones is of industrial importance, as it is a prerequisite for developing operation and control procedures that circumvent their formation. The formation of transversal temperature patterns in packed-bed reactors is also of intrinsic academic interest. In a fixed-bed reactor, the ratio between the characteristic diffusion time of the temperature and reactant concentration is smaller than unity. This is in contrast to the classical Turing pattern formation [2] that occurs in a two-variables diffusion–reaction systems when this ratio exceeds unity [3]. As explained in more detail in Section 2, this contradiction is limited to reactions with simple kinetics.

Spatiotemporal pattern formation is a ubiquitous phenomenon. Standing and spiral waves and moving fronts are

* Corresponding author. Tel.: +1 713 743 4305.
E-mail addresses: Dluss@uh.edu (D. Luss), cermsll@tx.technion.ac.il (M. Sheintuch).
[1] Tel.: +972 48292823.

0920-5861/$ – see front matter © 2005 Elsevier B.V. All rights reserved.
doi:10.1016/j.cattod.2005.02.043

some of the many patterns that have been observed in various biological (such as slime molds) and physiological systems (such as heart and brain activity) and others [4,5]. Most previous studies of pattern formation in chemically reacting systems were of homogeneous (typically liquid-phase or combustion gas-phase) systems [6]. Heterogeneous catalytic systems, used under atmospheric or higher pressure, have some unique features: their local activity and transport properties are inherently non-uniform, the boundary conditions typically affect them because of the long-range impact of the enthalpy balance. Moreover, the interaction between the solid- and fluid-phases can create and stabilize states, which would not exist in its absence. Previous reviews of the subject were presented by Slin'ko and Jaeger [7], Sheintuch and Shvartsman [8], Luss [9] and Kiss and Hudson [10]. We review here experimental and theoretical studies of the formation of spatiotemporal temperature patterns on catalytic surfaces and in packed-bed reactors. While these studies shed some light on the conditions leading to the formation of hot spots, there exists as yet no established guideline how to prevent hot zone formation in a packed-bed reactor. Hopefully, the review will stimulate studies that will generate these important rules. The review will address the major findings, but is not a comprehensive review of all the relevant studies. Thus, we apologize in advance to the researchers whose contributions are not covered here. We limit the scope to high-pressure studies, in which thermal effects are always important. Ertl and Imbihl [11] reviewed pattern formation in catalytic systems under ultra-low-pressure. Hudson and Tsotsis [12] and Krischer [13] reviewed oscillations and patterns in electrochemical systems.

2. Experimental observations

Spatiotemporal patterns have been observed in several heterogeneous catalytic systems. Many of these benefited from insight gained by extensive theoretical studies and numerical simulations of non-linear dynamic systems. We review here these experiments according to the geometry of the system in which they occurred.

2.1. Electrically heated catalytic wires and ribbons

Electrically heated catalytic wires and ribbons enable a rapid and easy control of their average temperature and determination of the heat generated by the chemical reaction. Thus, they have been used in many studies of various catalytic reactions. Langmuir [14] conducted some of his pioneering studies using such wires. Davies [15] observed that in certain cases electrically heated wires, on which a catalytic reaction occurred, may consist of two sections with a high and a low temperature. The two regions are separated by a sharp temperature front. Measurements by Barelko's group in Chernogolovka [16,17] of the temporal average wire resistance revealed that these temperature fronts are not always stationary; that finding motivated an analysis of the velocity of these temperature fronts [16].

The development of modern IR cameras enabled direct measurements of the temporal temperature profile on catalytic surfaces. The research group of Schmitz [18,19] was the first to use this experimental technique. They observed both stationary and spatiotemporal patterns on a single and an array of catalytic pellets during hydrogen oxidation. Lobban et al. [20] used IR imaging to determine the stationary temperature profiles obtained during the oxidation of ammonia on a thin electrically heated Pt ribbon, kept at a constant wire resistance, i.e., constant average wire temperature. They found that for certain average wire temperatures the wire may attain either a uniform temperature state or a non-uniform one. Fig. 1 shows such a case in which either a uniform or non-uniform temperature state can be obtained depending on the initial conditions. Obviously, the temperature of the high (low)-temperature region exceeded (was lower than) that of the average temperature. These experiments provided an experimental proof that global coupling (the control of the average wire temperature in this case) can stabilize non-symmetric temperature patterns, which would be unstable in its absence. A detailed analysis of the impact of global coupling is presented in Section 2.

In many theoretical studies, a no-flux condition is assumed to exist at both ends of a long wire. The stability of that system is affected by these boundary conditions, and the state of the system will be either homogeneous (uniform temperature), or a moving front that separates two regions with different temperatures. However, end-effects always are present in experimental systems (Fig. 1). Thus, we consider states which are either symmetric or asymmetric.

When catalytic experiments are carried on a thin wire heated electrically by a constant voltage, the pattern

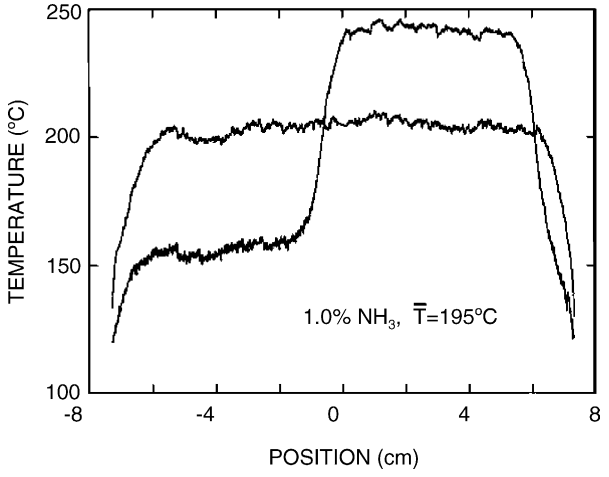

Fig. 1. The temperature profiles obtained during the oxidation of a mixture of ammonia (1 vol.%) in air on a Pt ribbon heated electrically so that its average temperature is kept at 195 °C. In this case, the initial conditions determine if a uniform temperature state or one with a stationary front is obtained (after Lobban et al. [20]).

formation is very similar to that under constant total resistance [21]. The reason is that under both modes of operation, the electrical heating stabilizes the sharp temperature front that separates the high- and low-temperature regions and counteracts any changes caused by movement of the front. The bifurcation diagram of the heat generation rate as a function of the ribbon voltage during the oxidation of a mixture containing 1.0% ammonia is shown in Fig. 2. A branch of non-uniform states existed over a bounded range of voltages. Within that region increasing the voltage increased (decreased) the size of the high (low)-temperature region. The current required to maintain these stationary non-uniform states was essentially independent of the voltage, i.e., the size of the high-temperature region.

When an oscillatory chemical reaction is carried out on an electrically heated ribbon, kept at a constant average resistance, non-symmetric oscillatory or chaotic states may be attained. Philippou et al. [22] found that during propylene oxidation on an electrically heated ribbon, the resistance of which was kept constant, the temperature fronts bounding the hot zone moved back-and-forth. The leading and trailing fronts moved at different velocities. The dynamic changes in the size of the hot zone and its temperature generated both periodic and chaotic states. The chaotic states were often associated with the splitting of the hot zone into two regions, which moved at different velocities. The oscillations of the overall reaction in the chaotic region were at a much higher frequencies than those of the local temperature. Such a case is shown in Fig. 3. We show in Section 2 that this back-and-forth motion can be accounted for by the constant resistance electrical heating.

When the oxidation of propylene was conducted under constant voltage operation chaotic states were obtained in a bounded voltage range. These chaotic states were similar to those observed under constant wire resistance and were caused by the irregular back-and-forth motion of the fronts bounding the high-temperature region. A reconstruction of the chaotic attractor of such a case is shown in Fig. 4.

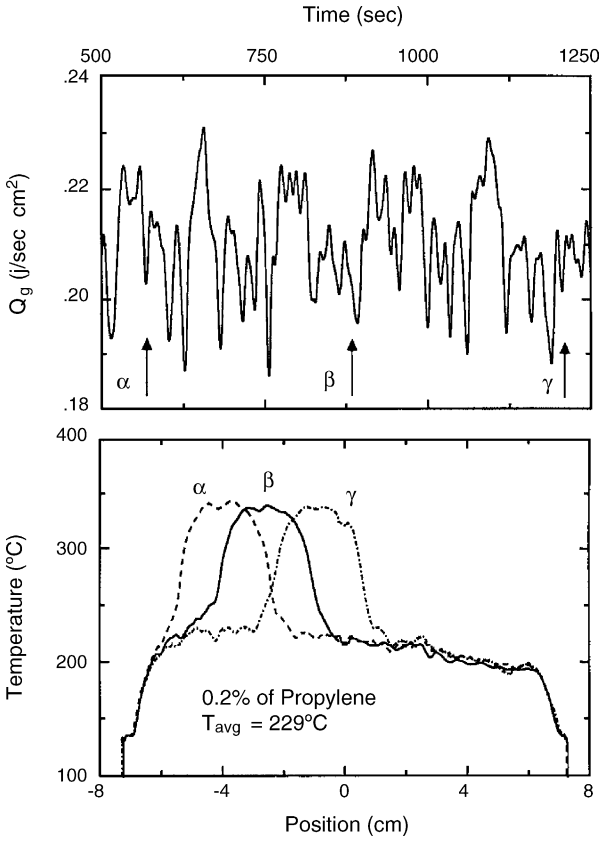

Fig. 3. Chaotic motion generated during the oxidation of a mixture of 0.2% propylene in air on an electrically heated wire kept at an average temperature of 229 °C. Top shows the temporal variation in the heat generated by the reaction. Bottom shows the temperature profiles of the back-and-forth moving temperature pulse during three instants (after Phillipou et al. [22]).

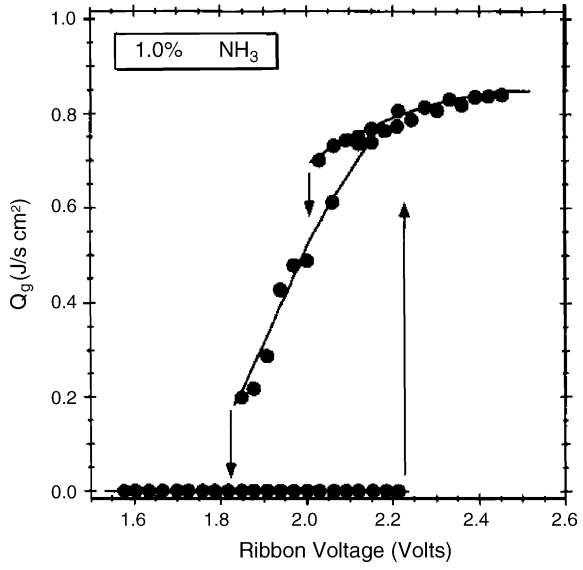

Fig. 2. The dependence of the heat generated by the chemical reaction on the constant voltage used to heat a thin Pt ribbon on which the oxidation of ammonia in air was conducted (after Phillipou and Luss [21]).

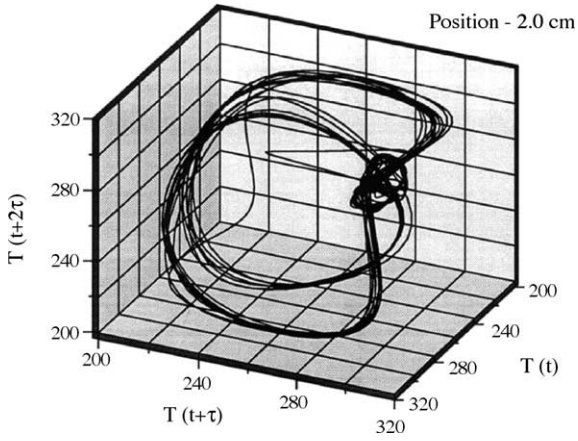

Fig. 4. A three-dimensional reconstruction of the attractor describing the local temperature on a thin Pt ribbon on which the oxidation of a mixture of propylene in air was conducted (after Phillipou and Luss [21]).

Theory predicts that when a reaction is conducted on a catalytic wire heated by a constant current its steady-state temperature should be uniform [23,24]. Sharp temperature fronts that can be induced by proper initial conditions are structurally unstable under this mode of electrical heating and propagate out of the system. For reactions the rate of which is single-valued at all temperatures, a stable stationary front separating a high- and low-temperature region is predicted to exist only for one current value. Barelko et al. [16] reported a surprising finding of a continuous range of electrical currents for which a stationary temperature front was obtained during the oxidation of ammonia. Phillippou and Luss [25] found later that the front had an exceedingly small velocity (order of 10^{-5} cm/s) over a range of currents, but that a stationary front existed only for one current, in agreement with the theoretical predictions. The relation between the underlying kinetics and the front properties are discussed in Section 2. We show there that a multi-step surface reaction mechanism can account for the apparently contradicting results described above.

A chaotic state generated by a back-and-forth movement of the temperature fronts bounding the high-temperature region, was observed by Phillippou and Luss [26] during the oxidation of propylene over a catalytic ribbon heated by a constant current. While that motion may have been caused by a transient change of activity, it is not clear what caused the front to stop and reverse its motion at the two ends of the ribbon. Both periodic and chaotic motions of hot temperature pulses on a Pt ribbon were observed by Schmidt's group [27,28] during the oxidation of ammonia. All these temperature pulses originated from a fixed point on the wire, which was not heated electrically.

Electrically heated wires and ribbons have been used to study the multiplicity and dynamic features of exothermic reactions and to extract kinetic parameters from these experiments [29–32]. The analysis of these experiments was conducted assuming that the wire's temperature was uniform. The potential existence of non-uniform states indicates that this assumption may lead to severe pitfalls in the analysis of these data.

2.2. Catalytic rings and cylindrical pellets

The behaviour of catalytic wires or ribbons is affected by the inevitable end-effects and the sojourn of moving pulses if the system is rather short. The need to circumvent these deficiencies and simplify the analysis and characterization led Mayer [33] to measure electrical pulse motion in a ring of jellyfish tissue rather than on a long rod. This idea motivated temperature measurements on catalytic rings and hollow cylinders. The first observation of a rotating temperature pulse during the catalytic oxidation of hydrogen on a thin Ni ring was by Graham et al. [34]. That pulse consisted of high-temperature zone, separated by narrow front from the low-temperature region. The corresponding time angular position dependence is shown in Fig. 5. The

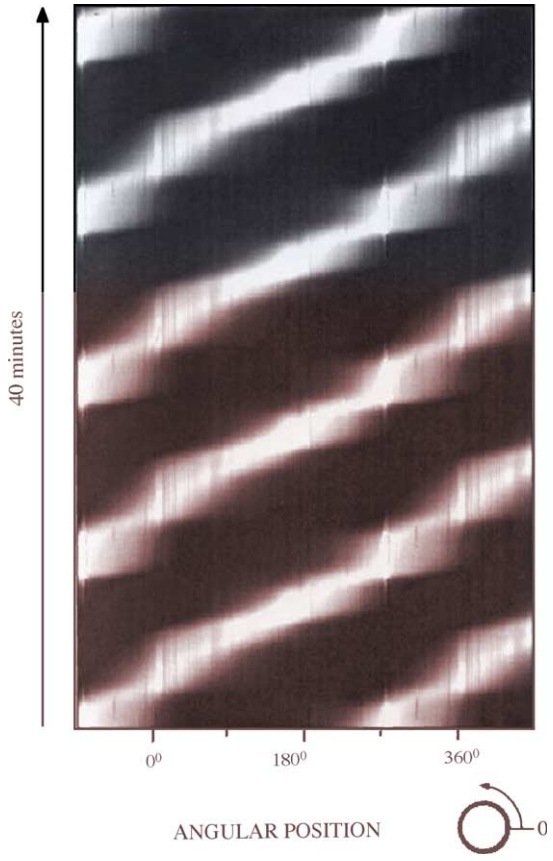

Fig. 5. A high-temperature pulse rotating on the surface of a nickel ring on which a mixture of H_2 (5 vol.%) and O_2 (95 vol.%) reacted. The white and black area corresponds to 390 and 255 °C, respectively. To help the view, the left- and right-hand of the edges overlap (after Graham et al. [34]).

measurements revealed that the pulse motion was periodic at any point, but its velocity and width depended on the azimuthal position. This motion differs from the constant velocity and shape motion of a pulse on a homogenous ring. This deviation was caused by the inherent non-uniformity of the catalytic surface and local variations of the transport coefficients in the reactor. Similar distortions of the shape and velocity of rotating pulses was observed in various other reacting systems. For example, it was noticed by Yamamoto et al. [35,36], Liauw et al. [37] and Annamalai et al. [38] during the oxidation of carbon monoxide. Graham et al. [39,40] found that even the anisotropic diffusion on a single crystal catalytic ring affects the azimuthal velocity of rotating concentration pulses under ultra-high-vacuum conditions. Bangia et al. [41] showed that controlled surface heterogeneities can strongly affect the concentration patterns of the surface CO concentrations when its oxidation is conducted on a single crystal kept at ultra-low pressures. The impact of surface non-uniformities has also been reported in several studies of pulses motion on rings in electrochemical systems [42–45]. Inherent non-uniformities and anisotropy are known to affect pattern selection and features also in many living systems. For example, patches of non-excitable scar tissue in the heart muscle affect the

local dynamics [47,48]. Theory predicts that the velocity of a pulse rotating around a uniform ring may be time-dependent, when the length of the ring is close to that at which a rotating pulse cannot exist [49].

Schmitz and Tsotsis [50] pointed out that mass and heat coupling among catalyst particles may generate stable spatial patterns. A comprehensive survey of the impact of coupling among particles in a ring was presented in [51]. Fascinating examples of the curious dynamics of general networks of coupled cells is presented in [52]. Experiments by Tsai et al. [53] and Wicke and Onken [54,55] showed that the coupling via the gas-phase between different sections of catalyst sections or between different catalyst particles can affect the steady-state and dynamic features of these systems and stabilize features that would not have occurred in the absence of this coupling. Both experimental [56,57] and theoretical studies [58,59] revealed that adsorbed reactants may form ''islands'' on smooth single crystals.

Ertl and Imbihl [11] have shown that the interaction between a catalytic single crystal and a mixture of carbon monoxide and oxygen may lead under ultra-low pressures to formation of many intricate spatiotemporal concentration patterns. The atmospheric experiments on the single catalytic rings and pellets revealed that both the moving and stationary hot regions are stabilized by global coupling. Specifically, any attempt of the hot region to expand decreases the concentration of the limiting reactant in the gas-phase and this arrests the front motion. It is worth noting that also in electrochemical systems global coupling has been shown to be a major contributor to pattern formed on rings [42–44]. While anti-phase (standing wave) oscillations were observed under globally coupled constant current (galvanostatic) condition, pulse motion was observed under potentiosatic conditions during anodic nickel dissolution [59].

Middya et al. [60] pointed out that the global coupling between the catalytic surface and the reactant gas-phase is the mechanism that enables temperature patterns to form and be stable on catalytic surfaces. The global coupling is equivalent to a space average control, which may generate intricate patterns and bifurcation among them [61]. Reactants mixing is not crucial for oscillations to emerge but may be crucial for pattern formation. Mixing can be viewed as a high rate of diffusion. The classical Turing pattern formation mechanism occurs in a two-variable reaction–diffusion system, containing an activator and inhibitor with a sufficiently large ratio of their diffusivities. Modelling of catalytic systems often requires accounting for more than two variables. The relation between their time scales and diffusivities that leads to evolution of spatio-temporal patterns cannot be classified in a simple way (see Section 2). As explained in Section 2, gas-phase mixing and its interaction with the catalytic surface may in some cases induce and stabilize symmetry breaking, i.e., pattern generation. An example illustrating this is the finding that increasing the intensity of the mixing in a vessel holding a Ni catalytic ring enhanced the formation, stability and uniformity of the temperature pulses formed during the oxidation of hydrogen and caused them to rotate in the same direction as the impeller [62]. However, mixing may also in some cases preserve the symmetry by synchronizing the state on the surface. An example of such a case is when the reactant inhibits its consumption, such as during the oxidation of CO under fixed fluid-temperature conditions.

The non-uniformity of catalytic rings tends to increase with time and change the dynamic features of the temperature patterns. The evolving non-uniformities may cause the pulses to slow down at some positions and even reverse their direction of motion [34,62]. In some cases, the non-uniformities caused a periodic *domain oscillation* in which the pulse was stationary for sometime and then moved rapidly to the other side of the ring. It stayed at that position for some time before returning to the original position. Various other motions were observed. Fig. 6 describes a situation in which a nearly uniform low-temperature state existed for some time before a hot spot formed from which two temperature fronts emanated and moved in opposite directions. When the hot zone occupied almost the whole ring, the two fronts reversed their direction leading to extinction. In some cases, a temperature pulse formed alternatively at either one of two locations, while the average ring temperature remained essentially constant. While

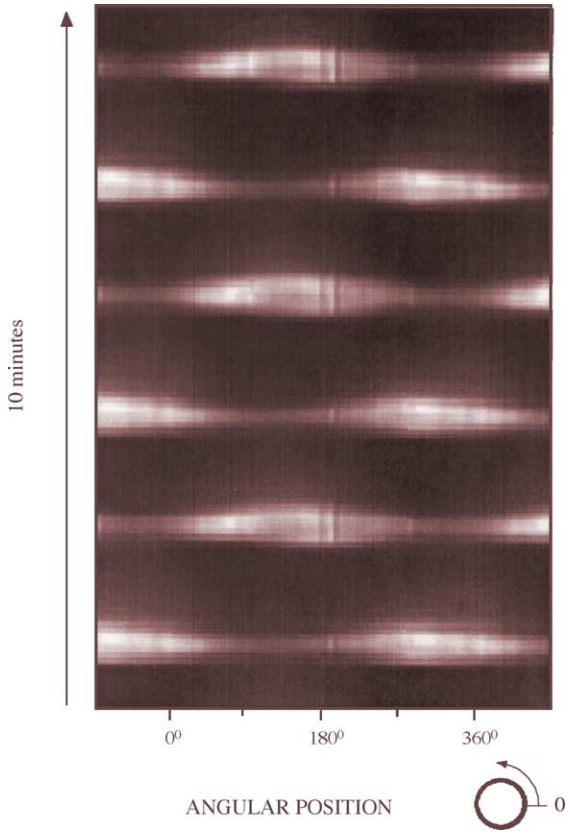

Fig. 6. Periodic formation and extinction of a hot region on a nickel ring on which a mixture of H_2 (5 vol.%) and O_2 (95 vol.%) reacted. The white and black areas correspond to 390 and 280 °C, respectively (after Graham et al. [34]).

various spatiotemporal patterns were observed during the oxidation of hydrogen on a suspended nickel ring catalyst, a stationary hot zone was formed when the same reaction was conducted using a thin ring of nickel supported on alumina [63].

While the ring geometry is very useful to study spatiotemporal pattern formation, most commercial catalysts have a more complex geometry. One step towards investigation of pattern formation on more realistic geometries is the study of a hollow thin cylindrical catalytic pellet. It may be looked upon as a two-dimensional model system with periodic boundary conditions. Annamalai et al. [64] built a special conical-mirror reactor, shown in Fig. 7, that enabled measuring the temporal temperature distribution on both the outside and top of the pellet.

The temperature patterns on the walls of the cylindrical catalytic pellets were more intricate than those observed on a catalytic ring on which the same reaction was carried out. The non-uniform temperature states were again obtained close to extinction. Following cooling of the reactor, a transition from a uniform fully ignited state to a non-uniform one occurred. Fig. 8(i) shows some temperature patterns observed on the top of a thin hollow ring during the oxidation of carbon monoxide. A uniform ignited state existed when the reactor was at 100 °C. A transition to a non-uniform state occurred at 85 °C. Further cooling to 65 °C caused the hot zone to periodically split into two separate pulses, which later coalesced. The splitting of the hot zone led to periodic backfiring, shown in Fig. 8(ii). The cause of this backfiring motion can be understood by inspection of the transient temperature profiles shown in Fig. 8(iii). After a hot zone forms, the rate of the limiting reactant (CO) consumption at its centre exceeds the rate of reactant adsorption (which decreases with increasing temperature). This decreases the rate of heat generation and hence the centre temperature decreases. This, in turn, causes the hot zone to split into two hot regions. The smaller region eventually is extinguished, while the larger one becomes a single hot zone, which due to global coupling is equal in size to the original pulse.

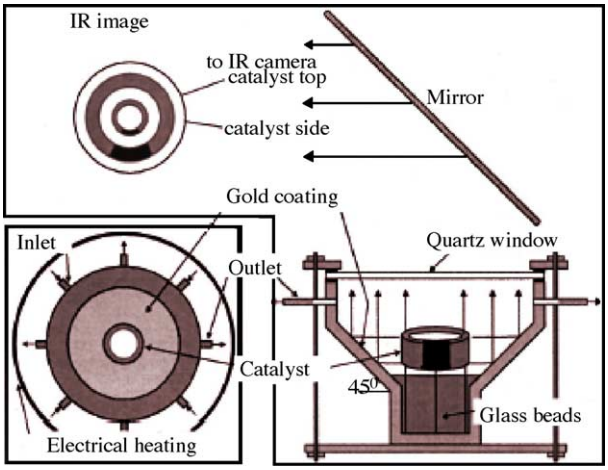

Fig. 7. A conical reactor designed to measure the temperature on both the top and side of a hollow cylindrical pellet by IR imaging. The radiation from the sides of the pellet is reflected by the gold plated conical walls to the mirror. The top of the pellet is seen as an inner ring, while the side is seen as an external ring (after Annamalai et al. [64]).

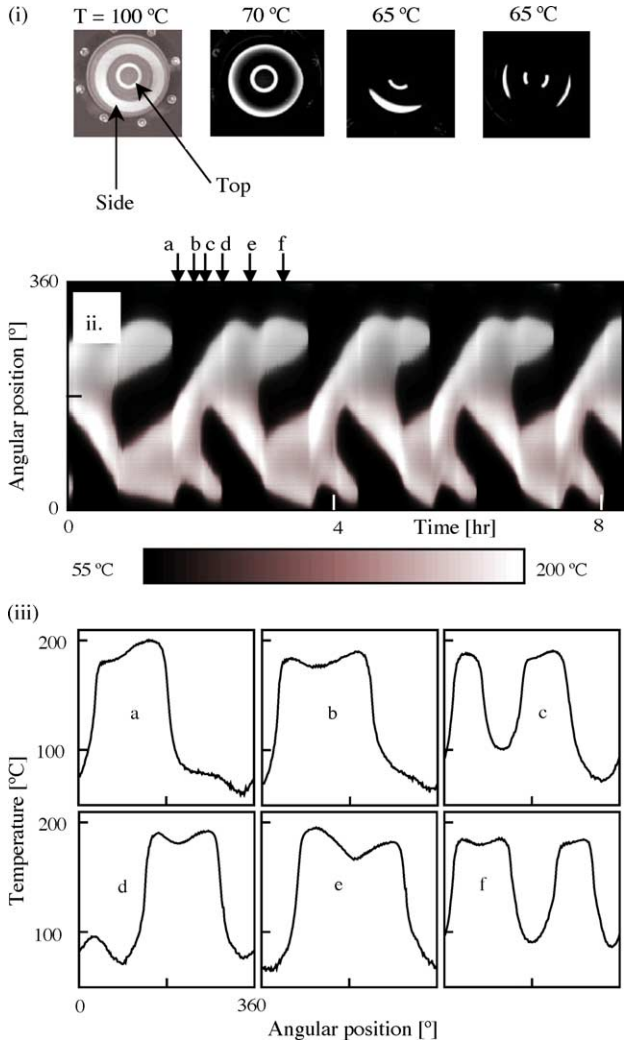

Fig. 8. (i) Snap shots of the temperature on the top of a hollow cylindrical catalytic pellet (Pd/Al_2O_3) during the oxidation of carbon monoxide for three reactor temperatures. (ii) The motion of the hot zone in the angular position–time plane at a reactor temperature of 55 °C. (iii) Instantaneous temperature profile at times corresponding to the arrows in (ii) (after Annamalai et al. [64]).

While the temperature patterns observed on the top of a thin hollow cylinder were qualitatively similar to those obtained on a thin ring, the temperature patterns on the pellet side were more intricate than those on a thin ring. The spatial temperatures on the side of the pellet are shown in Fig. 9 for three reactor temperatures. In several experiments, the temperatures on the top and bottom of the pellet were not the same. This was caused by the non-uniformity of the catalyst activity, the transport coefficients and the flow in the reactor. The splitting of the temperature pulse on the top of the pellet also occurred on its side in many experiments.

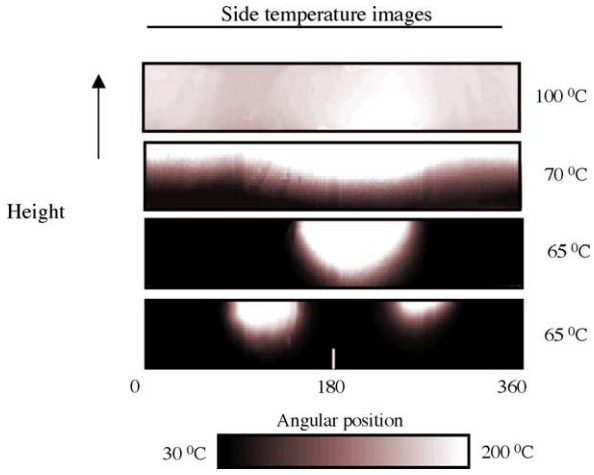

Fig. 9. Instantaneous temperature profiles on the side of the hollow catalytic pellet at three reactor temperatures. The two images at 65 °C correspond to those shown on the top of the pellet in Fig. 8(i) (after Annamalai et al. [64]).

The experiments with the hollow pellet as well as those with the catalytic ring indicate that the temperature patterns were affected by both the global coupling and the non-uniformity of the catalyst. Global coupling can stabilize temperature fronts and patterns that would not exist in its absence and counteract changes in the vessel concentrations. The non-uniformity led to formation of patterns that are different and richer than those obtained in uniform media.

Rather complex temperature patterns have been observed by Schmitz's research [18,19,65] in their pioneering IR imaging of the temperature on catalytic spherical pellets during hydrogen oxidation. However, they did not study the temporal features of the motion and the patterns were affected by the contact with the support and adjacent particles. The research group of Wolf used IR imaging to study the temperature patterns in the direction of the gas flow during the oxidation of ethylene and CO on a Rh/SiO_2 catalytic wafer [66–68]. They noted that a hot temperature zone periodically expanded, changed shape and contracted, while the reaction rate underwent sustained oscillation. The amplitude of the oscillations in the rate of CO_2 formation were correlated with the size of the hot zone [66,67].

2.3. Catalytic reactors

We describe patterns observed in catalytic packed-bed reactors in which the convection in the axial direction generates temperature and concentration gradients in that direction. Local hot spots are known to occur within industrial packed-bed reactors, as evident from the finding of fused catalysts (clinkers) when replacing of the catalyst from trickle-bed reactors used to conduct hydro-desulfurization [1]. There are numerous reports of the axial temperature profiles in packed-bed reactors under either steady-state or transient conditions. However, there are only very few reports of periodic temperature wave motion in packed-bed reactors, the feed to which is time invariant. These intricate travelling waves tend to appear when the dynamics of some catalyst particle are either oscillatory or excitable. For example, Puszynnski and Hlavacek [69] observed a periodic formation of a travelling hot spot in a packed-bed during the bed (Fig. 10). Wicke and Onken [54,55] observed similar periodic, travelling temperature waves in a packed-bed reactor during the oxidation of either CO or ethylene. They pointed out that these periodic temperature waves form when the reaction rate of the catalyst in the upstream section of the reactor is oscillatory. Rovinski and Menzinger [70] observed a periodic sequence of concentration pulses when they conducted out the oscillatory Belousov–Zhabtinski reaction in a catalytic packed-bed reactor.

Wicke and Onken [54,55] concluded from temperature measurements at two locations at the same cross section of the reactor that the reaction rate and temperature may vary periodically also in the radial direction, i.e., spatiotemporal transversal (normal to the flow direction) temperature patterns may exist in the bed. Identification and classification of the possible pattern requires many more transversal temperature measurements. Unfortunately, there are almost no published data of transversal temporal temperatures inside packed-bed reactors. Matros [71] reported the temperature field in the outlet of a packed-bed used for the partial oxidation of isobutyl alcohol on copper oxide catalysts. His measurements indicated the existence of several hot zones in the bed and that the temperature was strongly dependent on the azimuthal position (Fig. 11). However, repacking of the bed revealed that the presence of these hot zones was caused by non-uniform packing of the catalyst. Thus, these data do not enable any analysis of a potential impact of the interaction between the reaction, transport rates and convection on the formation of transversal hot regions.

IR imaging of the temperature field at the exit from packed-bed reactors provided information on temperature patterns on various types of shallow laboratory packed-bed reactors. Unfortunately, this experimental technique does

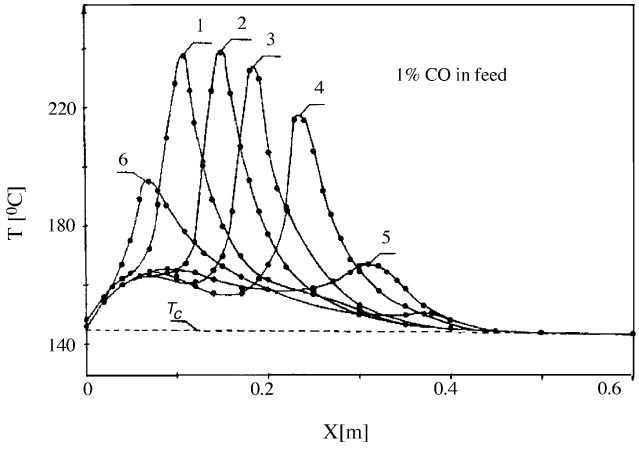

Fig. 10. Periodic travelling temperature waves in a packed-bed reactor in which the oxidation of CO was conducted. Numbers denote successive times at which profiles were measured (after Puszynski and Hlavacek [69]).

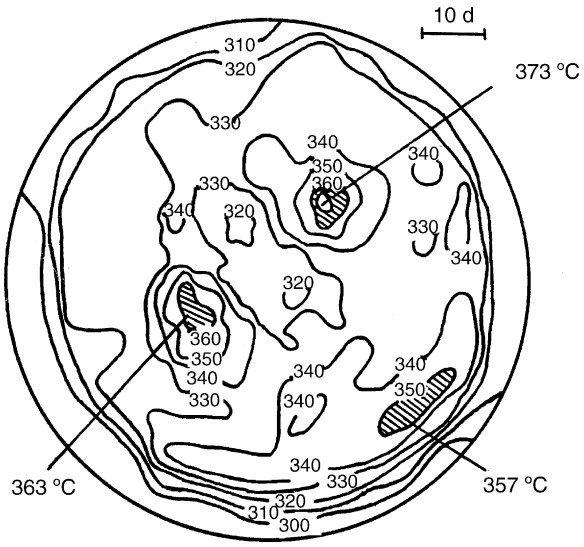

Fig. 11. Isotherms at the exit of a 120 mm long bed of copper oxide catalyst used to oxidize isobutyl alcohol. This highly asymmetric temperature field was due to non-uniform packing of the reactor (after Matros [71]).

not enable detection of local heat regions inside the bed and the temperature field on top of a long bed does not provide reliable information about the presence of hot zones well below the top. Qualitatively similar temperature patterns were observed at the exits of three types of packed-bed reactors in which carbon monoxide was oxidized: a radial-flow reactor [72], a shallow bed of catalytic pellets [73–75] and a catalytic glass-fiber cloth [76].

The main difference among these experiments was that the motions on the glass-fiber cloth reactor were much faster than those in the reactors packed with solid catalysts. Typical thermograms of sustained patterns during CO oxidation, with the feed flowing through the catalytic glass-fiber disks are shown in Fig. 12. The experiments revealed, among others, the presence of a hot spot that expanded and contracted continuously (a breathing motion) in a temporal fashion that matched the effluent CO_2 concentration. Rapid (period of about 1 min) oscillations were superimposed on the active phase of the long (10–60 min) cycle of complex relaxation oscillation. Simulations of the dynamics of a catalytic cloth, assuming that the gas-phase above the catalyst is mixed, are presented in Section 2 suggesting that the breathing motion emerged due to the heat loss to the ring holding the disc-shaped catalyst. In the absence of this wall, heat loss homogeneous oscillations are predicted to emerge. A period-adding mechanism can explain the change in the number of small peaks that appeared upon varying the operating conditions (reactor temperature).

In radial-flow and shallow-bed reactors, high- and low-temperature zones formed close to the extinction of the ignited, uniform temperature state. The sharp temperature fronts that separated the high- and low-temperature regions were in general non-stationary. The size of the high-

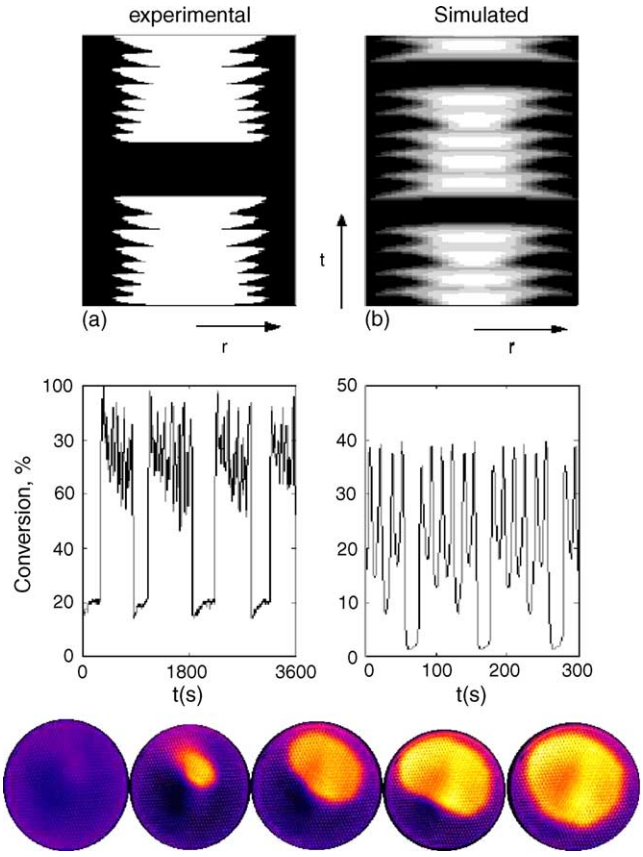

Fig. 12. Comparison of experiments (a) and simulations (b) of thermal patterns during CO oxidation on a disk-shaped catalytic cloth: upper row shows a gray scale spatiotemporal presentation of the (square root of the) active fraction on the surface. Middle row presents CO_2 effluent concentration indicating the three time scales of the problem. A typical oscillatory breathing pattern showing a sequence of snapshots over one peak (40 s) is shown in the lower row (1.4% CO in feed, 0.35% Pd/GFC catalyst; after Digilov et al. [76]).

temperature zone decreased as the temperature of the vessel containing the reactor was lowered. Following cooling of the ignited state a hot zone formed which underwent periodic expansion and contraction (breathing motion). In some cases the breathing caused periodic emission of a daughter small hot zone that eventually coalesced with the larger parent zone. Following additional cooling of the reactor, the hot zone exhibited an anti-phase motion (Fig. 13), i.e., the hot zone periodically occupied opposite sides of the area [75]. Additional cooling caused the hot zone to rotate around the reactor. Various complex types of rotations were observed. In some cases, the hot zone periodically rotated in one direction and then reversed its direction of rotation. Close to the extinction the hot zone often exhibited a "hopping" motion, in which the hot zone periodically rotated and then remained stationary for a while. In some hopping motions, the hot zone was stationary once every rotation. In other cases, it became apparently stationary twice or three times during each rotation [75]. An example of such a hopping motion is shown in Fig. 14.

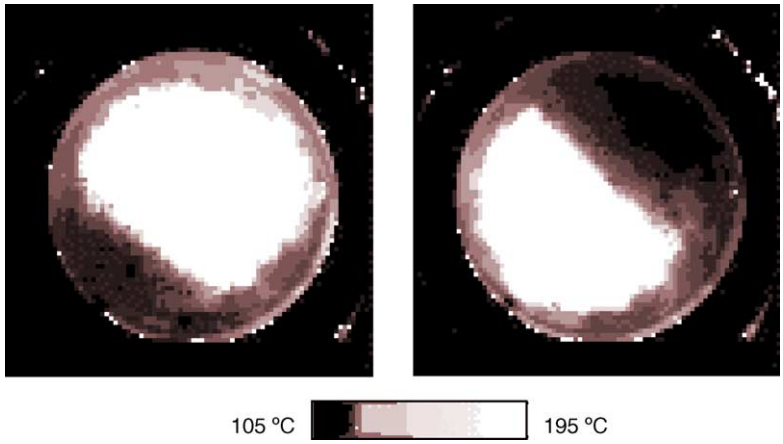

Fig. 13. Anti-phase motion on top of a shallow packed-bed reactor (catalyst Pd/Al_2O_3) during the oxidation of carbon monoxide (after Marwaha et al. [75]).

All the reported IR imaging of the temperature patterns on the top of a shallow packed-bed reactor were conducted using the oxidation of carbon monoxide as the test reaction. Recent unpublished experiments conducted in our laboratory indicate that similar patterns may be obtained also when other exothermic reactions are conducted in the reactor. The experiments with shallow reactors led to the finding of hot zones and their intricate motion. However, they have not yet provided a conclusive insight into what operating conditions or reactions and interactions are causing the formation of these hot zones within the bed. This insight is essential to develop operating and control procedures that circumvent their occurrence. Experimental information about the formation and dynamics of hot spot inside a long reactor may provide the needed missing insight about what causes their formation in industrial reactors and guidance about how to circumvent their evolution.

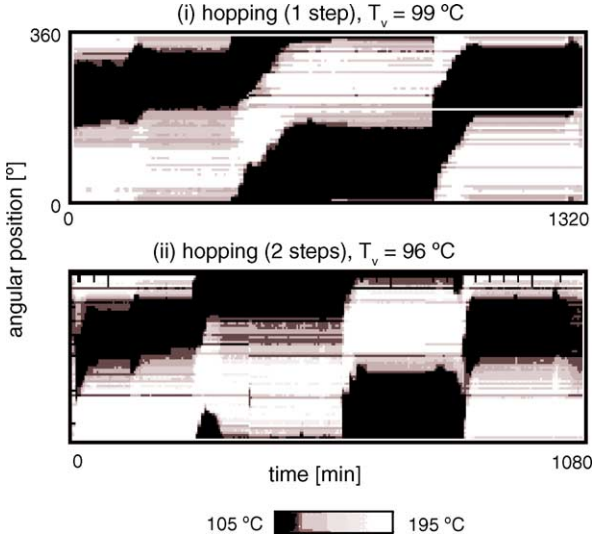

Fig. 14. A one-step (i, $T_v = 99$ °C) and two-steps (ii, $T_v = 96$ °C) hopping motion on top of a shallow packed-bed reactor (catalyst Pd/Al_2O_3) during the oxidation of carbon monoxide (after Marwaha et al. [75]).

3. Mathematical models: prediction and analysis

3.1. Introduction

We describe here recent developments in simulations, analysis and modelling of catalytic patterns. We only briefly address the issues of oscillatory mechanisms and kinetic models, which have been extensively reviewed (e.g., Slin'ko and Jaeger [7]). We concentrate mainly on spatial patterns due to the interaction of kinetics and transport (diffusion, conduction, convection). We differentiate between reaction–diffusion and reaction–convection–diffusion (either of species or heat) systems. The purpose of this review is to build a menagerie of these motions in order to use them in identification of experimental results and to understand the interaction among the various rate processes (kinetics, flow pattern) that causes their evolution. Hopefully, this information will enhance our understanding and prediction of these phenomena. In many cases, however, we are not able to make a complete classification of the possible dynamic features and may have to build a model specific to a certain system in order to test it. Patterns can be understood in many cases in terms of propagating fronts and we review the relation between the model structure and front motion.

3.2. Catalytic reaction–diffusion systems

Spatiotemporal structures usually emerge due to the interaction of oscillatory or multi-stable kinetics, with reactant diffusion and/or heat conduction. By oscillatory kinetics we imply that the smallest catalytic unit (a crystallite or a pellet) exhibits time-dependent oscillations when exposed to a constant reactant environment. The dynamic features of catalytic oscillations have been a subject of intensive research for many years and a plethora of mechanisms have been suggested (e.g., [7,77,78]). There is still no general agreement on the mechanism inducing catalytic oscillations. Early models (in the 1970s [79]) tried to explain this behaviour by the coupling of heat and mass

balances, which is the source of instabilities in gas-phase combustion and chemical reactions in a cooled CSTR. It became clear, however, that this approach cannot account for observations due to the large heat capacity of the catalyst, and the source of oscillations is, probably, complex kinetics. A simple way to produce oscillations is to couple an autocatalytic variable (an activator, x), that can attain stable multiple steady-states in a certain domain of parameters, with a slow inhibitor (y). A simple form of such a model is $x_t = f(x, y)$, $y_t = \varepsilon g(x, y)$, where $f(x, y) = 0$ is S-shaped (e.g., like $-x^3 + x - y = 0$) and ε is sufficiently small. Bistability in catalytic systems may result either from the enthalpy balance or from complex kinetics, as in CO oxidation [80]. When $f = 0$ and $g = 0$ intersect at an unstable steady-state oscillations evolve with a period of order $1/\varepsilon$. Thus, we can adjust the slow step to match the observed period.

The simplest pattern is a front, formed in a reaction–diffusion model of the form $x_t - \mathrm{d}^2x/\mathrm{d}z^2 = f(x, \lambda)$ with a bistable $f(x)$ and constant λ. Under proper initial conditions, a front forms that connects the upper solution (x_+), of $f(x_+, \lambda) = 0$, to the lower one (x_-). It propagates at a velocity $c(\lambda)$, that depends on a parameter (λ). The upper (lower) domain expands if $\int f(x)\,\mathrm{d}x > 0$ ($\int f(x)\,\mathrm{d}x < 0$, the integration is between the two stable solutions). The front is stationary only for $\lambda = \lambda_0$ that satisfies the Maxwell construction

$$\int_{x_-}^{x_+} f(x, \lambda_0) = 0. \tag{1}$$

When $f(x)$ is single-valued, there exists just one value that sustains a stationary front and, typically, the front propagates out of the system. Incorporating another balance that relates λ and x may enable a stationary front to exist for a bounded range of λ.

The best-known mechanism for pattern formation in reaction–diffusion systems is that by Turing [2]. Patterns may emerge in the diffusion–reaction system, $x_t - \mathrm{d}^2x/\mathrm{d}z^2 = f(x, \lambda)$, $\delta\lambda_t - D\,\mathrm{d}^2\lambda/\mathrm{d}z^2 = h(x, \lambda)$, when the diffusion of the inhibitor (λ) is sufficiently larger than that of the activator (x) ($D > 1$). As the front of x moves it affects the state of the fast diffusing λ. As it inhibits x it arrests the propagation of the activator front. Linear stability analysis predicts the intrinsic wavelength of the emerging pattern. For sufficiently large systems, the pattern is insensitive to the system size.

The Turing mechanism, however, does not apply to most catalytic systems. The typical inhibitor in catalytic systems, a surface concentration, is slowly diffusing or is non-diffusing. Moreover, inspection of the experimental results does not reveal an intrinsic wavelength and the boundaries always seem to affect the resulting pattern. Thus, we focus our attention on reaction–diffusion systems with a localized inhibitor. Such systems are unlikely to form stationary patterns. They may admit transient travelling pulse solutions or sustained homogeneous oscillations in a one-dimensional medium. Sustained moving pulses may emerge on a ring and spiral wave solutions on a disk, but only with special inhomogeneous initial conditions. The interaction of bistable or oscillatory kinetics with global coupling or with long-range interaction of a third variable may induce sustained patterns in systems with a localized inhibitor. The latter interaction is similar in principle to that in the Turing mechanism. It may be induced by mixing of the reactant fluid-phase or by a global control mechanism. As outlined in Section 2, a significant effort has been made to analyze such systems. Other effects, like patterns due to non-uniformities, are briefly discussed.

3.2.1. Models

Most analytical predictions presented here are for two- or three-variable systems. The behaviour of a many-variable system may exhibit new features, as shown below.

We consider here a simple model that describes spatiotemporal patterns and incorporates three variables: a fast activator (x), a localized and slow inhibitor (y) (i.e., $\varepsilon \ll 1$), representing a surface concentration, and a fast responding ($\delta \ll 1$) and fast-diffusing ($D \gg 1$) fluid variable (λ) that provides long-range or global interaction. The system is typically described by

$$\begin{aligned} &\text{(a)}\ x_t - \Delta x = f(x, y, \lambda); \qquad \text{(b)}\ y_t = \varepsilon g(x, y, \lambda); \\ &\text{(c)}\ \delta\lambda_t - D\,\Delta\lambda = h(x, y, \lambda) \end{aligned} \tag{2}$$

and is subject to either no-flux or Dirichlet's (or mixed) conditions at its perimeter. Δ is the Laplacian operator.

Global and long-range interaction: if the fluid variable (λ) is assumed to be well-mixed ($D \to \infty$) then λ is space-independent and depends on the spatial average reaction rate on the surface. Its temporal and length scales are scaled with respect to those of the activator. We consider cases in which $\delta \to 0$, so that λ responds to changes much faster than the catalyst variable (x). We also assume that $\varepsilon \ll 1$, so that y may be assumed to be in pseudo-steady-state. The main effect of a strong global λ interaction is to eliminate either the homogeneous oscillatory or stationary solution.

Global interaction may be induced by gas-phase mixing. Enthalpy and mass mixing may generate opposing effects, as communication of heat tends to synchronize the system. Mixing may induce symmetry-breaking interaction when the fluid temperature in the reactor remains constant due to heat loss, while the catalyst temperature can vary (Middya et al. [61]). We define the interaction to be symmetry breaking (symmetry-preserving) if local ignition or extinction (upward or downward jump in x) at one edge of the catalyst inhibits (accelerates) the same process elsewhere. Qualitative analysis reveals that mixing of reactants consumed by positive-order kinetics induces symmetry breaking, while in negative-order reactions it preserves the symmetry. In reactions like CO oxidation on Pt or Pd the reaction order varies with gas-phase concentrations and the nature of the interaction may vary.

(i) The simplest model system exhibiting fronts and pattern formation due to global coupling is that with

polynomial kinetics of the lowest order:

$$f(x,y,\lambda) = -x^3 + x + y + \lambda; \qquad g(x,y) = (-\alpha x - y); \qquad h(x) = b(x + x_0) \tag{3}$$

The parameter b determines the nature of interaction between the global- and local-variable. $b < 0$ ($b > 0$) corresponds to symmetry-breaking (-preserving) interaction. This learning model does not correspond to any actual reaction. It qualitatively agrees with our understanding of the thermokinetic oscillatory systems, as explained in the next paragraph. Extensive studies of one-dimensional systems showed that these polynomial kinetics predict patterns that are quite similar to those predicted by thermokinetic models. This simple model obeys certain symmetries, and its predictions enable pattern classification. Several of its asymptotic cases, including the fixed λ case, have been analyzed in detail. In the case of strong global coupling, integrating the fluid-phase balance (Eq. (2c)) and incorporation of the boundary conditions yields, $\langle x + x_0 \rangle = 0$, where $\langle \cdot \rangle$ denotes a space averaged value. That implies that the upper steady-state occupies a fixed fraction of the surface (half when $x_0 = 0$).

(ii) The simplest model that accounts for thermal effects, that are always present in high-pressure experiments, is that of a first- (or positive-) order exothermic reaction coupled with a slow inhibitor (y) that is activated at low temperatures and deactivated at high temperatures. This *thermokinetic oscillatory* model can be described by Eq. (2) with $x = T$. The heat balance assumes that the catalyst (a wire, gauze or cloth) is thin and its temperature (T), which is distributed in space, differs from that of the fluid (T_a) that is assumed to be constant. The heat balance accounts for accumulation (τ_T is the time scale), conduction (L_T is the length scale), heat generation by the reaction, $R(T, y, c)$, and heat transfer to the fluid. If the reaction kinetics is of positive-order then the mass balance over the reactant surface concentration (c) can be expressed as a function of both y and T and incorporated into R. The resulting energy balance is of the form

$$\tau_T \frac{\partial T}{\partial t} - L_T^2 \nabla^2 T = aR(T,y) + (T_a - T) = f(T, y, T_a) \tag{4}$$

If $R(T)$ is sigmoidal then $f(T, y) = 0$ is shaped like the cubic $f(x, y) = 0$ (Eq. (3)). The dynamics of the slow variable (y) was discussed in [78]; in its simplest form it can be set to be linear in T and in y. The similarity of the phase plane behaviour accounts for the dynamic similarity of the polynomial kinetics model (Eqs. (2) and (3)) and the thermokinetic model. This commonality was described in detail in appendix of [81].

An electrically heated wire may be described approximately by Eq. (4), where T_a is modified by the current. Using a control to keep the wire at a constant resistance, keeps the average wire temperature at a preset value, $\langle T \rangle$, while manipulating the control variable (actuator), T_a. The current, which is space-independent, induces global coupling with symmetry-breaking interaction.

(iii) The two-variable models described above are quite simple and their qualitative behaviour can be predicted even when global interaction is important. The description of most catalytic reactions requires a more detailed model. The simplest kinetic model of CO oxidation on group VIII metals should incorporate three steps: dissociative oxygen adsorption, CO adsorption and desorption and surface reaction. A surface micro-kinetic model that accounts for these three steps is (Turner et al. [82]; Slinko et al. [83])

$$\frac{d\theta_{CO}}{dt} = k_1 P_{CO}(1 - \theta_{CO} - \theta_O) - k_{-1}\theta_{CO} - k_3\theta_{CO}\theta_O - [k_5\theta_{CO}y];$$
$$\frac{d\theta_O}{dt} = k_2 P_{O_2}(1 - \theta_{CO} - \theta_O)^2 - k_3\theta_{CO}\theta_O - [k_4\theta_O(1 - y)] \tag{5}$$

where θ_{CO} and θ_O are the concentration of adsorbed carbon monoxide and adsorbed oxygen respectively, and all rate constants follow an Arrhenius temperature dependence, $k_i = k_{i0}\, e^{(-Ei/RT)}$. Under isothermal conditions such a model predicts multiple steady-state solutions and the oxidation rate ($R = R_{CO} \sim k_3\theta_{CO}\theta_O$) versus CO partial pressure (P_{CO}) diagram includes a clockwise hysteresis loop. Thus, in a one-dimensional (1D), isothermal system, we can produce infinitely many solutions in which the discontinuity in the surface state occurs at an arbitrary spatial position; note that the surface variables are localized (Eq. (5)). Thermal effects are long-ranged and always important in high-pressure studies. Coupling of this kinetics with a thermal balance (Eq. (4)) can produce stationary fronts over a bounded domain of operating conditions [84]. To produce oscillatory solutions we couple the (θ_{CO}, θ_O, T) model with a slow-changing variable (y). The slow variable is interpreted as the oxygen concentration in a subsurface layer and its balance accounts for surface oxidation and reduction,

$$\frac{dy}{dt} = k_4\theta_O(1 - y) - k_5\theta_{CO}y \tag{6}$$

These oxidation and reduction steps affect the CO and oxygen balances (the bracketed terms in Eq. (5)); the slow variable y is assumed to affect the adsorption rate of oxygen like $k_2 = k_2^0\, e^{-\alpha y}$ [83]. The kinetic parameters employed in the examples below were suggested by Slinko et al. [83].

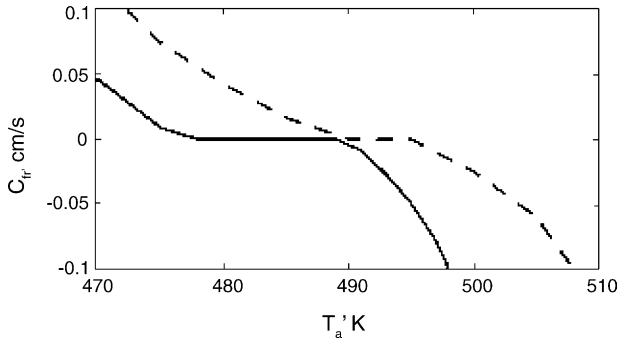

Fig. 15. Temperature-dependence of front velocity in a wire using a detailed kinetics model (P_{CO} = 300 Pa, solid line, or 400 Pa, dashed line); a domain of stationary front is evident (after Nekhamkina and Sheintuch [84]).

3.2.2. Classification of patterns

Eqs. (2) and (3) can admit an extremely rich plethora of patterns. The solutions are highly sensitive to the initial conditions and their symmetry. Patterns of polynomial kinetics may be classified by their symmetries (see [85]), but the distinction in other models is not as sharp as in the polynomial kinetics model.

3.2.2.1. Reaction–diffusion systems under local-coupling. We review here the main dynamic features of models that are not subject to global interaction.

Fronts: As explained in Section 2.1, single-variable one-dimensional systems (Eqs. (2) and (3), $y = 0$, fixed λ) may admit travelling wave solutions in which the upper (lower) state is expanding when $\lambda > 0$ (<0). Stationary fronts exist only at $\lambda = 0$, the boundary between the two regimes. The thermal balance exhibits similar results (Eq. (4), fixed y, T_a): the ignited (extinguished) domain expands at high (low) T_a.

The detailed kinetics model with fixed P_{CO}, y (i.e., when the lumped system (Eqs. (4) and (5)) admits bistability) can predict structurally stable stationary fronts in a one-dimensional system, so that such fronts exist over a bounded domain of temperatures or gas-phase concentration: Fig. 15 presents three such domains with expanding ignited zones (large T_a), stationary fronts (intermediate T_a) and expanding extinguished zones.

Wires and rings: Two-variable one-dimensional models (fixed λ; sometimes referred to as a Fitzhugh Nagumo type model) predict, with proper initial conditions, transient patterns like moving fronts or moving pulses that eventually settle into either a homogeneous oscillatory or stationary solution. In homogeneous oscillations, the whole system oscillates uniformly (similar to Fig. 16c). These models cannot admit sustained patterns. In systems with a wide separation of time scales ($\varepsilon \ll 1$), the motion is determined by α (Eq. (3)). The corresponding phase plane can be classified as bistable, oscillatory or excitable. The thermo-kinetic–oscillatory model exhibits similar results.

A possible solution on a ring is a unidirectional (UD) pulse, which travels around the ring at constant velocity (similar to Fig. 18d). Its emergence requires special initial conditions; homogeneous stationary or oscillatory states are typically established with homogeneous initial conditions when global interaction is absent (Middya et al. [60]).

The oscillatory version of the detailed kinetics model (Eqs. (4)–(6), fixed P_{CO}), exhibits multi-front patterns on a wire or a ring with a characteristic wavelength (Fig. 16 [85]). We describe now the effect of increasing P_{CO} in this system, while maintaining a constant temperature. Beyond a Hopf bifurcation, a transition to moving waves occurs (Fig. 16a). The wave number near the Hopf bifurcation point can be predicted by linear stability analysis (from the neutral curve). This implies that a moving wave with the computed characteristic wavelength will emerge as the homogeneous state becomes unstable. This is not a Turing bifurcation. For large systems this wavelength is independent of the system size; the ring perimeter in Fig. 16 (20 mm) was large with respect to this wavelength. Further increase of P_{CO} leads to

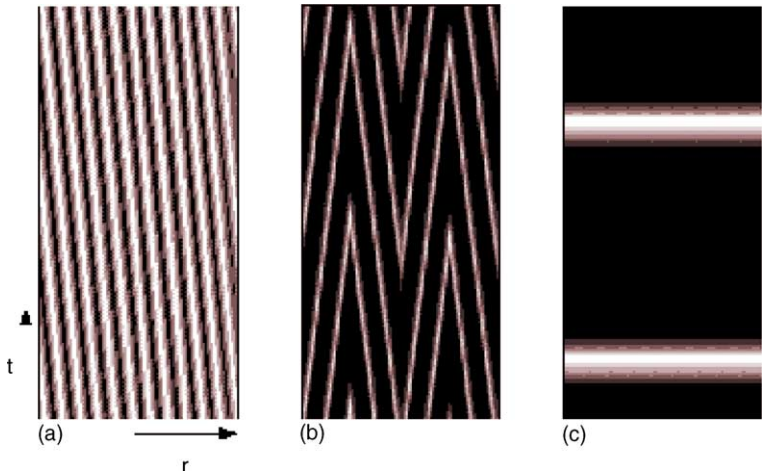

Fig. 16. Three typical patterns simulated in a ring using a detailed kinetics model showing travelling fronts (a, P_{CO} = 39 Pa), source and sink points (b, P_{CO} = 300 Pa) and homogeneous oscillations (c, P_{CO} = 500 Pa) (T = 480 K; after Nekhamkina and Sheintuch [86]).

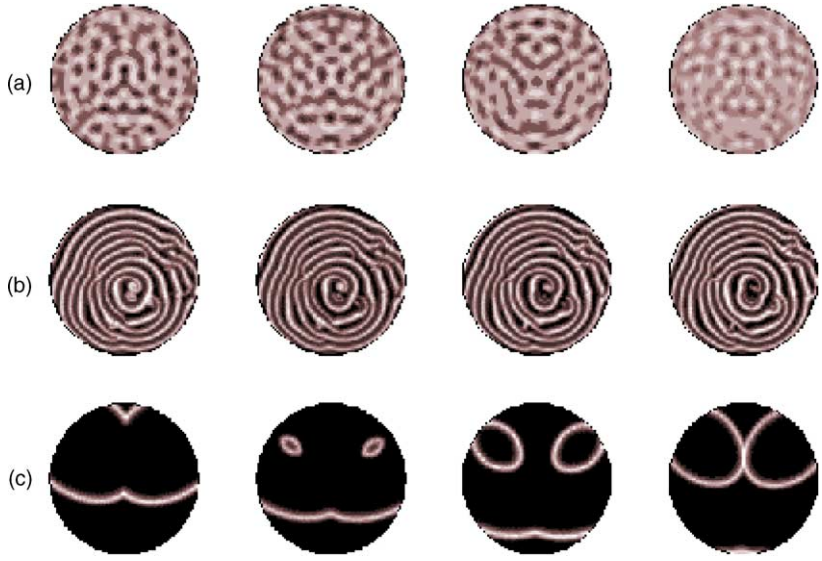

Fig. 17. Three typical patterns simulated in a disk using a detailed kinetics model showing travelling fronts (a, $P_{CO} = 39$ Pa), imperfect targets (b, $P_{CO} = 400$ Pa) and a source-point pattern (c, $P_{CO} = 450$ Pa) ($T = 480$ K; after Nekhamkina and Sheintuch [86]).

source-point solutions (SP) solutions, in which two pulses appear and travel in opposite directions (Fig. 16b); eventually when a pulse meet another one, they annihilate each other and disappear. Further increase leads to homogeneous oscillations (Fig. 16c) and then to another Hopf bifurcation.

Disks: Extensive simulations of two-variable (x, y) two-dimensional uniform systems typically reveal either target-patterns or spiral waves [5] that form under special initial conditions. The velocity of the fronts depends on their curvature. These results apply also to the thermokinetic oscillatory model described above.

The detailed-kinetics model, can exhibit a much richer behaviour. In analogy to the patterns on a ring (Fig. 16), increasing P_{CO} leads to the following patterns on a disk (Fig. 17): small amplitude cellular patterns (Fig. 17a) appear near the Hopf bifurcation point, imperfect multi-wave target patterns (Fig. 17b) appear at higher P_{CO} and moving pulses (Fig. 17c) appear in a domain where source point solutions were observed on a ring (Fig. 16b). All these patterns are obtained with fixed P_{CO}. Mixing of the gas-phase in a reactor, may destroy some of these patterns [84].

3.2.2.2. Reaction–diffusion systems subject to global coupling. Motions on a wire or ring: A single-variable bistable system subject to global interaction ($D \to \infty$) admits structurally stable fronts (Pismen [23]). To illustrate this consider a constant resistance control of a wire (Eq. (3)), i.e., a constant $\langle T \rangle$. An expanding ignited zone leads to larger $\langle T \rangle$ and consequently the external control decreases the heating current, which in turn arrests the front. The front is arrested with an effective T_a value that satisfies the Maxwell condition (Eq. (1)). Changing the set-point will affect the front position but not the effective T_a. Now, $\langle R \rangle \sim \langle T \rangle - T_a$ (Eq. (4)) which explains the experimental observations in Figs. 1 and 3. Both figures demonstrate that for ammonia

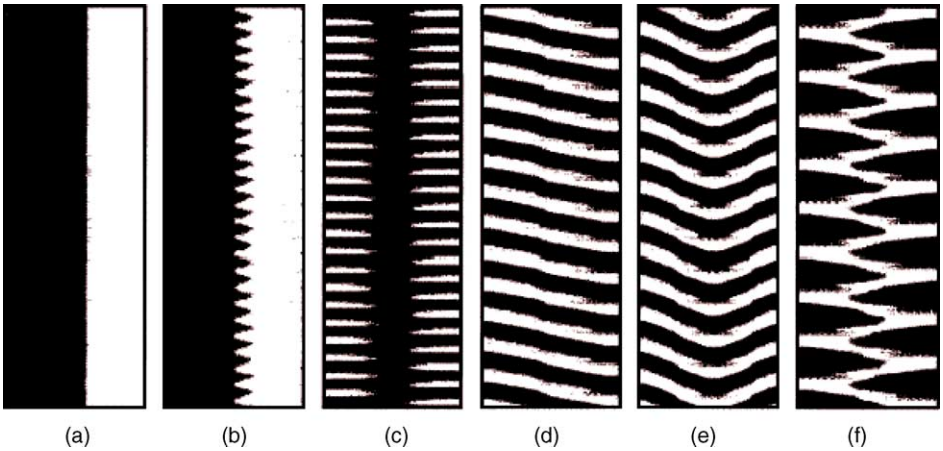

Fig. 18. (a–f) Spatiotemporal patterns simulated with polynomial kinetics for globally coupled wires (after Middya et al. [85]).

oxidation under certain conditions we can obtain either a non-uniform state with a stationary front or a homogeneous state, both states have the same average temperature. The analysis of the constant voltage control (employed in Fig. 3) is similar to that of constant resistance. A detailed analysis, including the effect of the heat loss at edges and wire length was presented by Sheintuch and Schmidt [24].

Middya et al. [60] classified the possible solutions of the polynomial model according to their symmetry (Fig. 18). Motions on a wire can be classified either as stationary fronts or moving pulses. A single front may be either stationary or oscillatory (Fig. 18a and b). It may undergo anti-phase (standing wave) oscillations, in which two sections oscillate out of phase (Fig. 18c). A wire or a ribbon with global interaction is unlikely to sustain motions that incorporate two or more stationary fronts. If the system initially contains several fronts, they will coalesce in a process similar to Ostwald ripening. Moving pulses on a wire include the unidirectional pulse, which is born at one edge of the system and travels and exits at the other (Fig. 18d), and the back-and-forth pulse (BF, Fig. 18f). The system may also admit source-point or sink-point (NP) states, in which a pair of pulses either appear or disappear (Fig. 18e). The bifurcation diagram, obtained upon changing a parameter like the system length, includes a complex sequence of transitions between the two pairs of BF and UD pulses [60,85]. A discrete version of this problem, with N identical subsections subject to global control, was analyzed by Sheintuch [87]. The moving pulse solution in Fig. 2 can be accounted for by the model above; its similarity to the BF pulse pattern (Fig. 18f) is evident, except that part of the wire does not participate in the motion, probably due to its inactivity.

When the homogeneous states are unstable due to global interaction then the UD pulse is the most likely pattern to be established on a ring [60]. Other motions that exist on a ring, coexist with the UD pattern. The UD pattern explains the behaviour in Fig. 4. The global coupling effect of the gas-phase was discussed in Section 1. The observed time-dependent velocity may be accounted for non-uniformity of the catalytic activity or by operating close to the boundary where a moving pulse solution disappears (e.g., Qu et al. [49] determined the bifurcation diagram near that boundary for a ring of cardiac cells).

Motions on a disk and cylinder: Motions on a disk subject to global control were studied by Sheintuch and Nekhamkina [89] using Eqs. (1) and (2) with $x_0 = 0$ and varying D, which determines the pattern wave number, and by Middya and Luss [88] for infinite D and varying $\lambda = B(x - x_0)$, the strength of the global coupling. Most of the classification below assumes $x_0 = 0$; in that case the system admits inversion symmetry: i.e., if $[x(t), y(t), \lambda(t)]$ is a solution so is $[-x(t), -y(t), -\lambda(t)]$ or, in other words, interchanging the black and white sections of the patterns presented below is also a solution.

Stationary patterns: Fig. 19 shows several stationary front patterns that emerge in a bistable system (i.e., Eqs. (1) and (2), $y = 0$), for both global and long-range ($D = 100$) interaction. A close relation exists between the two and a sensitive dependence on the initial conditions. Several stationary waves, differing in wave number, may coexist in a one-dimensional system and it is not surprising that a large number of different solutions coexist on a disk in a bistable system. Note, again that the case of finite D corresponds to Turing patterns. The emergence of an intrinsic wavelength in the $D = 100$ case is evident.

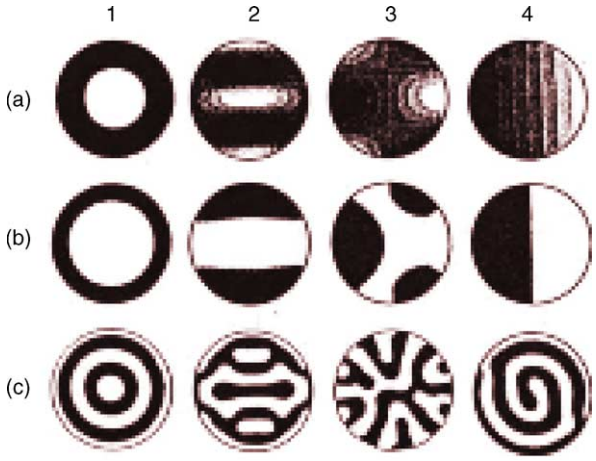

Fig. 19. Stationary states simulated with polynomial kinetics and $y = 0$ in a disk subject to global-range (row b) or long-range (row c, $D = 100$) interaction for various initial conditions (row a) (after Sheintuch and Nekhamkina [89]).

Spatiotemporal patterns: the three-variable (x, y, λ) system may exhibit target, rotating and other patterns; we limit the discussion, here, to global coupling (i.e., infinite D): *target* patterns include stationary target patterns, oscillatory target patterns in which the target diameter expands and contracts, and moving target patterns, that can propagate inwards or outwards. *Patterns with rotation symmetry* include: rotating spiral patterns (Fig. 20f, left) and rotating fronts (Fig. 20d). *Other patterns* that were simulated include oscillating fronts (Fig. 20a and e), moving pulse patterns (Fig. 20b), similar to unidirectional motions in one-dimensional systems, and two such pulses (Fig. 20c). The patterns in Fig. 20 were computed under global coupling with $x_0 = 0$. Relaxing the latter condition may lead to break-up of the spiral patterns and produce asymmetric (and typically chaotic) patterns (Fig. 20f shows four snapshots from the behaviours simulated with increasing x_0; Fig. 20a–e, each, present a half cycle simulated with $x_0 = 0$).

Motion on a cylinder: spatiotemporal patterns on a cylindrical catalytic surface subject to global interaction, were simulated in [90] using the polynomial kinetics model (Eqs. (1) and (2)). While for very short (small length L) or very narrow (small perimeter P) cylinders the pattern preserves the structures of the corresponding one-dimensional problems (a ring or a wire), two-dimensional patterns emerge for comparable L and P. The system exhibits a large multiplicity of spatiotemporal behaviour because of a very

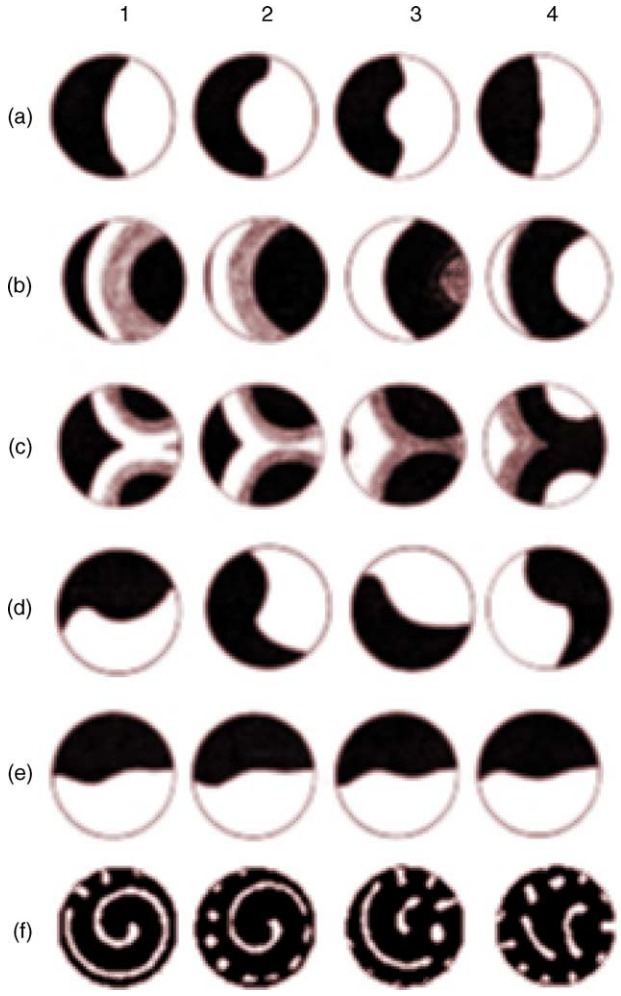

Fig. 20. Patterns simulated with polynomial kinetics in a disk subject to global interaction (after Sheintuch and Nekhamkina [89]); each row represents half-a-cycle: (a) $\alpha = 0.2$, (b) $\alpha = 0.45$, (c) $\alpha = 0.7$, (d) $\alpha = 0.2$, (e) $\alpha = 0.15$. Row (f) represents a transient break-up of spiral patterns with the loss of inversion symmetry (increasing of x_0, $\alpha = 0.2$).

high sensitivity to initial conditions. Approximate solutions for the bifurcation from one- to two-dimensional patterns were derived [90].

3.2.3. Comparing experiments and simulations

A mathematical model was constructed to account for the experimental IR thermography observations on the disk-shaped cloth catalyst in a continuous reactor with feed flowing perpendicular to and through the disk (Fig. 12) The model was based on the oscillatory kinetics model of Slinko et al. [83] (Eqs. (5) and (6)) coupled with an enthalpy balance (Eq. (4); the gas temperature was assumed to be constant, τ_T was estimated to be ~2 s, $L_T \sim 0.2$ cm), subject to a constant temperature at the boundary, and coupled with a mixed gas-phase concentration which provide communication across the surface [91]. A qualitative analysis suggested that the observed breathing motion emerged due to the interaction of the imposed cold-edge boundary condition that reflects the experimental conditions, with the non-linear kinetics. The mathematical model predicted the following observed features: (a) sustained breathing motion in which a hot spot expands and contracts continuously. (b) Temporally complex patterns that can be classified as mixed-mode oscillations with a large relaxation-type conversion peak on which several smaller peaks were superimposed (see Fig. 11 for comparison of experimental and simulated patterns). (c) A period-adding mechanism that accounts for the change in the number of smaller peaks with varying operating conditions (the reactor temperature). Simulations of the distributed system reveal the features described above as well as the nature of the bifurcation to complexity.

Note that the model employed here is identical to that used to produce Fig. 17, except that the gas-phase was assumed to be completely mixed (as opposed to fixed P_{CO}) and the rim temperature was assumed to be constant (versus no-flux in Fig. 17). Mixing the reactants induced symmetry-preserving interaction due to the negative-order kinetics and destroyed the patterns simulated for fixed P_{CO} in Fig. 17.

3.2.4. Concluding remarks

The three kinetic models presented in Section 2.1 do not exhaust all the possible motions in catalytic systems. Comparison of the two- and five-variables detailed kinetic models shows that new features, that are difficult to predict by qualitative or linear analysis, can be introduced by the incorporation of new variables even if they are localized. The study of polynomial kinetics was extended to a quintic source function (Eqs. (2) and (3) but with $f(x, y) = -x(x^2 - 1)(x^2 - a^2) + y + \lambda$), that qualitatively describes the behaviour of catalytic oscillations with two simultaneous or consecutive reactions [92]; a richer class of solutions was found in this case than that predicted by a cubic source-function: most notably, under global interaction the system exhibits stable multi-front patterns.

Non-uniformities of properties, like catalytic activity and transport coefficients, are common in catalytic systems and were evident in studies of spatiotemporal patterns (Section 1 [34–39]). Under such conditions it is usually difficult to conclusively differentiate between the effects of spontaneous symmetry breaking and those due to non-uniformity. Analysis of the dynamics of one-dimensional systems with single- or two-variable kinetics and space-dependent properties showed that these systems may admit stable stationary-fronts, oscillatory fronts, source-points and unidirectional pulses even in the absence of global coupling [93]. Other effects of non-uniformities, in catalytic, electrochemical or living systems, are listed in Section 1 [39–48].

While we have used continuous models to describe these systems, catalysts are typically discrete in nature. Each reactor (order of 1 m in size) is packed with pellets (that are few mm in size), which in turn include metal crystallites (10–100 nm in size) that act as the catalytic sites (0.25 nm in

size). The behaviour of discrete systems may qualitatively differ from those of continuous systems, for example, fronts may become stationary over a domain of parameters; its size may diminish with the number of cells in the system [115,118]. Experimental studies [53–55] of catalyst particles were reviewed in Section 1. The behaviour of a population of non-uniform globally coupled systems (i.e., catalytic particles that interact only through the gas-phase) is currently a subject of intensive research [119–121]: if the coupling is strong and the parameter dispersion (non-uniformity) is small, the particles will evolve almost in phase. In the opposite case, the elements of the population move incoherently and their behaviour is averaged out. Between these two asymptotic cases, complex collective behaviours arises, including oscillator death in which all particles states are steady. One example of oscillations over a line of nanoparticles embedded in a zeolite matrix was numerically investigated [128].

While global or long-range interaction can lead to an amazing array of new patterns, using it in order to account for experimentally observed pattern requires justification of the physical coupling. That may be justified in controlled resistive heating but gas-phase mixing effects do not always lead to symmetry breaking, as pointed out in Section 2.3.

3.3. Patterns due to convection, conduction and reaction

3.3.1. Introduction and modelling

While catalytic reaction–diffusion patterns may not be as rich and diverse as those in liquid-phase reaction, they appear in a class of reactions of significant commercial importance. The working-horse of the process industry is the fixed-bed and it is important to be able to predict spatiotemporal patterns in these reactors. Reactor-dynamics and steady-state multiplicity of packed-bed reactors catalyzing an *n*th-order exothermic reaction have been extensively studied [116]. Transient phenomena like creeping fronts [94,95], wrong-way behaviour [96,117] have been simulated and observed. Sustained oscillatory behaviour have been predicted for homogeneous (typically combustion) reactions, but were not found in simulations of packed-bed reactors due to the large heat capacity [97].

Axial (in flow direction) pattern development in one- and two-dimensional (cylindrical) reactor models with oscillatory kinetics are described below. Also described in this section is symmetry breaking in the transversal direction [98–100] using a thermokinetic (non-oscillatory) model of a fixed-bed. We do not review here patterns due to recycle or due to recuperating of enthalpy in the flow-reversal [100,101], counter-current [101], internal-recycle [102], loop-reactor [103,104] or ring-reactor [105]. These reactors sometimes produce patterned solutions, due to external or internal feedback. These reactors may generate patterned states even in the absence of oscillatory kinetics.

Several kinetic models were employed in the study of axial pattern formation in a fixed catalytic bed, for reactions with oscillatory kinetics: starting with a polynomial kinetics (Eqs. (2) and (3)) with convection of λ [81], then with a single thermokinetic oscillatory reaction [106,107] and finally with a detailed kinetics model. Pattern selection is determined by the kinetics and reactor models and by the nature of the fronts. The kinetics of oscillatory systems can usually be classified according to their phase plane. This tool cannot be used in the fixed-bed, as the phase plane varies along the reactor, since the fluid concentration and temperature change with axial position.

The homogeneous or heterogeneous one-dimensional reactor models, in which an exothermic catalytic reaction of first-order activated kinetics, $r = Ay\,\mathrm{e}^{-E/RT}C_\mathrm{A}$, is conducted, can be written in the following form [106,107]:

$$\begin{aligned}
&\frac{\partial x_1}{\partial \tau} + \delta\frac{\partial x_1}{\partial \xi} - \frac{1}{\mathrm{Pe_C}}\frac{\partial^2 x_1}{\partial \xi^2} \\
&= \mathrm{Da}\cdot y(1-x_1)\exp\left(\frac{\gamma x_2}{\gamma + x_2}\right) + \beta_\mathrm{C}(X - x_1) \\
&= f_1(x_1, x_2, y) \\
&\mathrm{Le}\frac{\partial x_2}{\partial \tau} + \delta\frac{\partial x_2}{\partial \xi} - \frac{1}{\mathrm{Pe_T}}\frac{\partial^2 x_2}{\partial \xi^2} \\
&= B\cdot \mathrm{Da}\cdot y(1-x_1)\exp\left(\frac{\gamma x_2}{\gamma + x_2}\right) + \beta_\mathrm{T}(Y - x_2) \\
&= f_2(x_1, x_2, y)
\end{aligned} \tag{7}$$

where x_1 and x_2 are the conversion and dimensionless temperatures, and y is the catalyst activity. We use the conventional notation for dimensionless parameters (B is the reaction exothermicity, Da the activity, γ the activation energy, Le the heat capacity and $\mathrm{Pe_T}$ or $\mathrm{Pe_C}$ are the dimensionless conduction or mass-dispersion).

The homogeneous model assumes that interphase gradients of temperature and concentration are absent. It is described by Eq. (7) with $\delta = 1$ and $\beta_\mathrm{C} = \beta_\mathrm{T} = 0$. The Danckwert's boundary conditions are typically imposed on the model

$$\begin{aligned}
&\xi = 0, \frac{\partial x_1}{\partial \xi} = \mathrm{Pe_C}(x_1 - x_{1,\mathrm{in}}), \quad \frac{\partial x_2}{\partial \xi} = \mathrm{Pe_T}(x_2 - x_{2,\mathrm{in}}); \\
&\xi = 1, \quad \frac{\partial x_1}{\partial \xi} = \frac{\partial x_2}{\partial \xi} = 0;
\end{aligned} \tag{8}$$

When heat- and mass-transfer resistance between the two phases cannot be ignored then the solid-phase of the heterogeneous model is described by Eq. (7) with no flow terms, $\delta = 0$. In an adiabatic reactor, the fluid variables, X and Y, which vary along the reactor are described by

$$\varepsilon\frac{\partial X}{\partial \tau} + \frac{\partial X}{\partial \xi} = \beta_\mathrm{C}(x_1 - X); \qquad \varepsilon\frac{\partial Y}{\partial \tau} + \frac{\partial Y}{\partial \xi} = \beta_\mathrm{T}(x_2 - Y); \tag{9}$$

To obtain oscillatory behaviour, the above equations are coupled with slow reversible changes in the catalytic

activity (y) ([87,108] $\tau_y \partial y/\partial\tau = -(M/\gamma)x_2 - (1+K)y + K \equiv g(x_2, y)$, where M and K are parameters).

The comparison of steady-state behaviours of the homogeneous and heterogeneous reactor models has been a subject of several investigations. These were typically aimed at finding a simple transformation of the parameters that enable prediction of the behaviour of the heterogeneous model using the homogeneous one [109,122].

A secondary target of the study of a heterogeneous oscillatory model [107] was to extend this transformation for oscillatory solutions. Analysis showed that the Vortmayer parameter-conversion approximation ($1/\mathrm{Pe}_{\mathrm{eff},i} = 1/\mathrm{Pe}_i + 1/\beta_\iota$, i = T or C, where β_ι is the external transport parameter) can predict quite well the dynamics of the heterogeneous model by a pseudo-homogeneous one when $\beta_\iota \gg \mathrm{Pe}_i$, but it fails when both parameters are comparable. While the Vortmayer approximation [109] is adequate when transport occurs between the two phases, it may lead to erroneous predictions in the presence of chemical reactions [122–124].

3.3.2. *One-dimensional pattern formed in flow direction*

The review below attempts to classify patterns formed in the flow direction in adiabatic homogeneous and heterogeneous reactor models, and the effect of β and Pe_T numbers on the emerging patterns. These patterns are formed by the interaction between front motion, fluid-flow and changing activity.

Almost homogeneous oscillations (almost periodic horizontal bands) emerge when the inlet dynamics is oscillatory (i.e., when the feed conditions induce oscillations in the absence of convection): that is the case for low β_T or low Pe_T. In patterns with $\mathrm{Pe}_\mathrm{T} \geq 100$ the fronts sweep the whole reactor (Fig. 21a). The almost synchronous nature results from the fast communication by convection and the symmetry-preserving nature of communication by enthalpy mixing. At larger Pe_T ($>10^4$) a stationary front periodically sends narrow pulses downstream (Fig. 21b). The dynamic behaviour of the homogeneous model yields surprisingly similar patterns. The difference between the two models become significant when $\beta_\mathrm{T} < \mathrm{Pe}_\mathrm{T}$.

When the phase plane corresponding to the inlet is an extinguished-state, the model exhibits a sharp front that oscillates around its stationary positions (Fig. 21d, $\mathrm{Pe}_\mathrm{T} = 3000$), while the exit may be ignited. Patterns are sustained over a relatively narrow domain of Pe_T numbers. The amplitude increases with decreasing Pe_T and at $\mathrm{Pe}_\mathrm{T} = 1000$ the front sweeps the whole surface (Fig. 21c).

Significant differences between the two models occur for small β_T values, around unity, for which $\beta_\mathrm{T} < \mathrm{Pe}_\mathrm{T}$. Fig. 22, upper row presents the complex aperiodic solid temperature behaviour, at the inlet (low-frequency) and the outlet of the heterogeneous model with $\beta_\mathrm{T} = \beta_\mathrm{C} = 1$ and $\mathrm{Pe}_\mathrm{T} = 500$. The corresponding pseudo-homogeneous model exhibits an extinguished steady-state.

Keren and Sheintuch [110] considered oscillations in the catalytic converter for CO oxidation on Pt using an oscillatory elementary-step model. It was found that due to the synchronous nature of the oscillations the lumped system still provided a good estimate of the oscillatory domain in the distributed system. The converter may exhibit either a stable steady behaviour or an oscillatory motion. In a typical oscillatory motion, which may be periodic or chaotic, a hot front enters the reactor exit and quickly moves upstream; extinction occurs almost simultaneously due to the strong coupling by convection (Fig. 22, lower row). Recent automotive converter designs employ resistive heating to expedite the start-up of a cold converter. Such heating can be applied locally, in order to produce a travelling front, or globally (using a metallic monolith) to heat up the whole reactor or its part. New avenues of cold-starting the converter, which is an excitable system, by means of periodic local perturbations were studied. The analysis shows, however, that this approach is not advantageous due to the slow relaxation of the surface activity during CO oxidation. The problems of light-off of the converter, for this highly exothermic and highly-

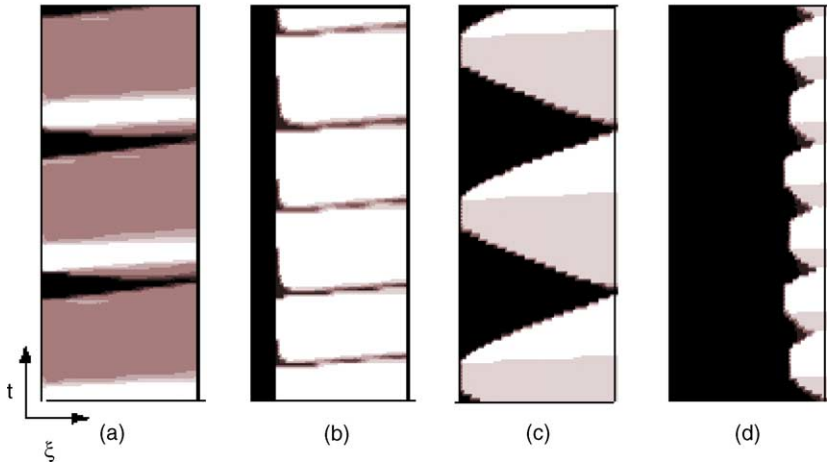

Fig. 21. Almost homogeneous oscillations (a and b) and oscillatory front solutions (c and d) simulated in an adiabatic heterogeneous reactor model when Pe and β are comparable; similar patterns were simulated with a pseudo-homogeneous model (after Sheintuch and Nekhamkina [107]; flow is from the left).

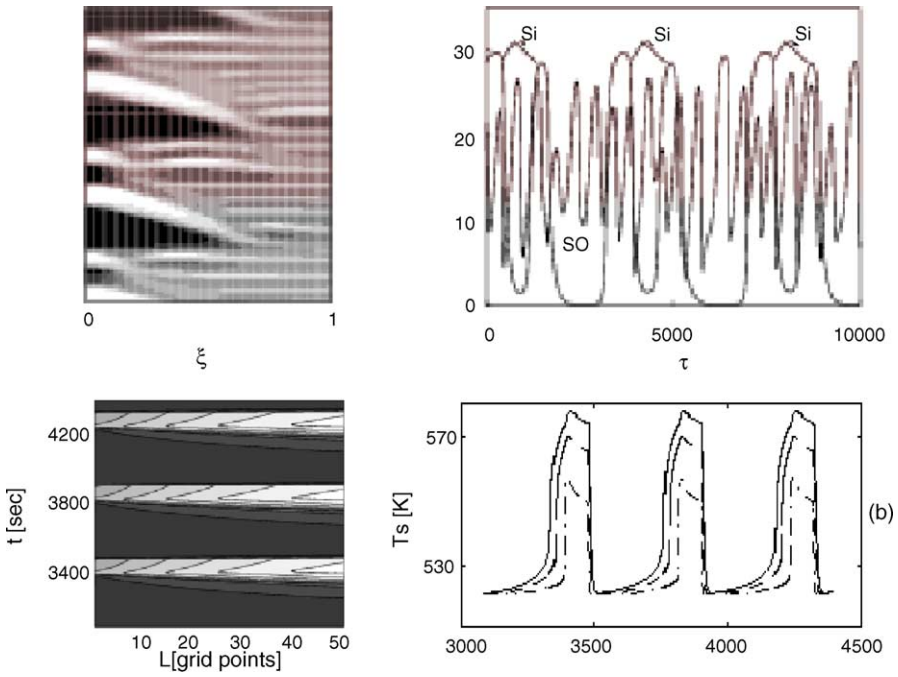

Fig. 22. Aperiodic patterns simulated with the heterogeneous reactor model at low β_T (upper row, $\beta_T = 1$, $Pe_T = 500$, after Sheintuch and Nekhamkina [107]; flow is from the left) and simple temporal oscillations of the catalytic converter showing the behaviour at the exit (lower row, after Keren and Sheintuch [110]). The left column presents the spatiotemporal behaviour of the solid temperature and the right column presents the temporal behaviour of the solid temperature at the inlet (s_i) or outlet (s_o).

activated reaction, was studied by Leighton and Chang [111]. They have also suggested a new converter design by increasing the catalyst load and decreasing the heat capacity of the entrance region.

3.3.3. Transversal patterns

Several studies addressed the emergence of patterns in the direction perpendicular to the flow. The studies described below used a homogeneous model of a fixed catalytic bed (the thermokinetic model, similar to Eq. (7)), with characteristically large Lewis and Peclet numbers, which may be coupled with slow changes of catalytic activity (i.e., oscillatory kinetics). Three-dimensional reactor models were studied by linear analysis and two-dimensional models were simulated numerically, one assuming angular symmetry and the other employing a cylindrical shell as a reactor model.

Balakotaiah et al. [98] used linear stability analysis to predict the isotherms for various transverse modes and to construct the neutral stability curves for a three-dimensional reactor with a Langnuir-Hinshelwood kinetics. The first four transverse modes to emerge are shown in Fig. 23a. The stability curves were calculated using $Pe_T = 50 = 5Pe_C$, i.e., $Pe_T > Pe_C$. This implies that the dispersion of the reactant (inhibitor) is larger than that of the temperature (activator).

Yakhnin and Menzinger [99] claimed that these patterns formation is due to a Turing-like interaction between the temperature and the concentration, which play the roles of activator and inhibitor. Thus, for such patterns to emerge, the heat dispersion should be smaller (or Pe_T larger) than that of mass. Their numerical simulations found a stable asymmetric pattern (Fig. 23b) for the parameter values used by Balkotaiah et al. [98]. The Turing analogy is just a qualitative suggestion, since it was derived for case in which no convection occurs. However, in practice, $Pe_h < Pe_m$, so these simulations do not correspond to the observations of transversal hot regions in packed-bed reactors. Recently, Viswanathan et al. [112] have proven that for a monotonic rate expression, such as an *n*th-order reaction, the patterns are unstable when $Pe_h < Pe_m$. This calls for further studies to determine the mechanisms generating these hot regions in commercial reactors.

Patterns due to oscillatory kinetics in reactors of high Le undergo symmetry breaking in the azimuthal direction of a cylindrically shaped thin catalytic reactor, when the perimeter is sufficiently large [113]. The generic regular patterns simulated then are rotating multi-wave patterns of constant rotation-speed (Fig. 24b exhibits one-, two- or three-wave patterns, for different perimeters) and oscillatory-'firing' ones, where the pattern fires hot-pulses as it rotates (Fig. 24c presents three snapshots). Their selection is highly sensitive to governing parameters and initial conditions. The results were organized in a bifurcation diagrams showing the coexisting 2D solutions with varying perimeter. Increasing convective velocity or reactor radius leads to symmetry breaking of regular patterns and the system may switch to chaos.

A similar study with polynomial kinetics model [114] revealed steady rotating band solutions, that emerge with proper initial conditions, and exist for sufficiently low fluid velocity *V* (Fig. 24a). The rotating solutions coexist with the

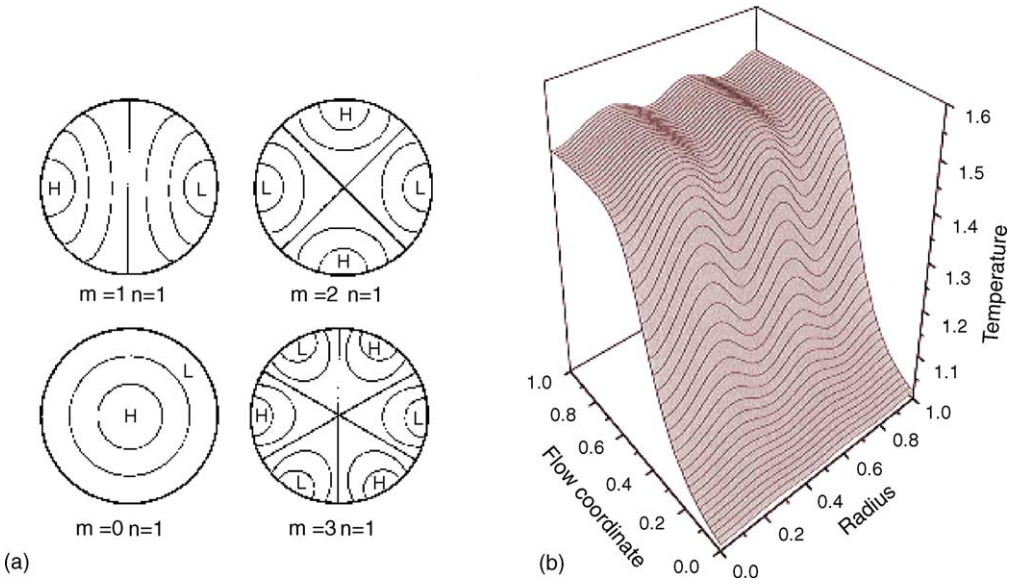

Fig. 23. Analysis and simulation of steady transversal patterns in the homogeneous reactor thermokinetics model: (a) first four transversal modes that emerge, as determined by linear analysis (after Balakotayah et al. [98]) and (b) simulated pattern in a bed with assumed angular symmetry (after Yakhnin and Menzinger [99]).

oscillatory solutions that are independent of the angular coordinate.

3.3.4. Impact of physical properties change

The physical properties of fluid may be a rather sensitive function of the temperature. Thus, temperature gradients may induce flow, which in turn may affect the temperature. In most reactor models, only the species and energy balance are considered and the momentum balance is not taken into account. This may lead to erroneous predictions of the state and stability of the reactor. For example, under constant pressure drop the flow rate and temperature in different tubes in multi-tube packed-bed reactor may not be the same in all tubes. Moreover, this may lead to formation of spatiotemporal patterns, as pointed out by Gatica et al. [127]. A more extensive investigation of this reaction-driven flow was conducted by Balakotaiah's research group [125,126].

The simulations suggest that this induced flow maldistribution is important mainly at very low flow rates, under which the impact of natural convection is dominant.

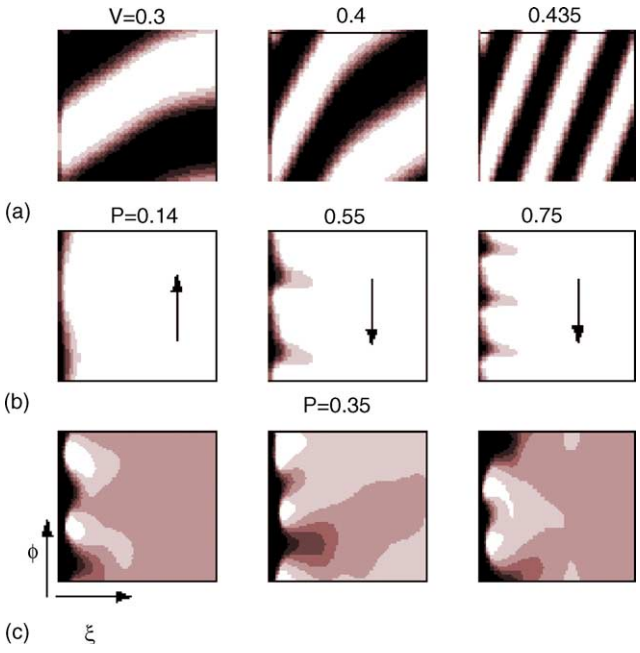

Fig. 24. Typical oscillatory transversal patterns in a cylindrical reactor. (a) First row shows rotating frozen patterns in the polynomial-kinetics model at increasing convection velocities (V) (after [114]). Rows (b) and (c) show rotating (one-, two- and three-wave) "frozen" and irregular "firing" patterns, correspondingly, simulated with the thermokinetic oscillatory model, at increasing perimeters (P) (high Le, varying activity and a low ratio of Pe_c/Pe_T, after [114]).

4. Closing remarks

Spatiotemporal patterns in heterogeneous catalytic systems are of intrinsic academic interest and of practical importance. Most pattern evolution studies were of homogeneous gas- or liquid-phase systems. The patterns generated in catalytic systems are usually of a different nature and the mechanisms that cause their evolution and stability differ from those in homogeneous reaction–diffusion system. They exhibit, however, behavioural features similar to those encountered in other heterogeneous systems such as electrochemical, solid-combustion and even physiological systems. These patterns are strongly impacted by global interaction, inherent heterogeneity of the system and interaction between different surface and sub-surface kinetics.

While advances have been made in the understanding of evolution of hot regions in packed-bed reactors, the reasons

leading to formation of local transversal hot regions have not yet been clearly established. It is important to gain an understanding of this phenomenon in order to be able to circumvent its occurrence and to assess its potential for a beneficial application.

Acknowledgements

We wish to acknowledge the support of this research by grants from the USA–Israel Binational Science Foundation, the NSF and the Welch foundation.

References

[1] C.H. Barkelew, B.S. Gambhir, ACS Symp. Ser. 61 (1984) 237.
[2] A. Turing, Philos. Trans. R. Soc. Lond. Ser. B 237 (1952) 37.
[3] L.A. Segal, J.L. Jackson, J. Theor. Biol. 37 (1972) 545.
[4] J.D. Murray, Mathematical Biology, Springer, Berlin, 1989.
[5] M.C. Cross, P.C. Hohenberg, Rev. Mod. Phys. 65 (1993) 851.
[6] R. Kapral, K. Showalter (Eds.), Chemical Waves and Patterns, Kluwer, Dordrecht, 1994.
[7] M.M. Slin'ko, N.I. Jaeger, Oscillating Heterogeneous Catalytic Systems, Elsevier, Amsterdam, 1994.
[8] M. Sheintuch, S. Shvartsman, AIChE J. 42 (1996) 1041.
[9] D. Luss, Ind. Eng. Chem. Res. 36 (1997) 2931.
[10] I.Z. Kiss, J.L. Hudson, AIChE J. 49 (2003) 2234.
[11] G. Ertl, R. Imbihl, Chem. Rev. 95 (1995) 697.
[12] J.L. Hudson, T.T. Tsotsis, Chem. Eng. Sci. 49 (1994) 1493.
[13] K. Krischer, in: B.E. Conway, J.O'M. Bockris, R.E. White (Eds.), Modern Aspects of Electrochemistry, vol 32, Plenum Press, New York, 1999, p. 1.
[14] I. Langmuir, Trans. Faraday Soc. 17 (1922) 621.
[15] W. Davies, Philos. Mag. 19 (1935) 3190.
[16] V. Barelko, I.I. Kurochka, A.G. Merzhanov, K.G. Shkadinski, Chem. Eng. Sci. 33 (1978) 805.
[17] Y. Volodin, V. Barelko, P.I. Khazlov, Chem. Eng. Commun. 18 (1982) 271.
[18] P.C. Pawlicki, R.A. Schmitz, Chem. Eng. Prog. 83 (2) (1982) 40.
[19] G.A. D'Netto, J.R. Brown, R.A. Schmitz, Ind. Chem. Eng. Symp. Ser. 87 (1984) 247.
[20] L. Lobban, G. Philippou, D. Luss, J. Phys. Chem. 93 (1989) 733.
[21] G. Phillipou, D. Luss, Chem. Eng. Sci. 48 (1993) 2313.
[22] G. Phillipou, F. Schulz, D. Luss, J. Phys. Chem. 95 (1991) 3224.
[23] L. Pismen, Chem. Eng. Sci. 35 (1980) 1950.
[24] M. Sheintuch, J. Schmidt, Chem. Eng. Commun. 10 (1986) 1513.
[25] G. Phillipou, D. Luss, Chem. Eng. Sci. 48 (1993) 2325.
[26] G. Phillipou, D. Luss, J. Phys. Chem. 96 (1992) 6551.
[27] G.A. Cordonier, L.D. Schmidt, Chem. Eng. Sci. 44 (1989) 1983.
[28] G.A. Cordonier, F. Schuth, L.D. Schmidt, J. Chem. Phys. 91 (1989) 1983.
[29] L. Hiam, H. Wise, S. Chaikin, J. Catal. 10 (1968) 272.
[30] S.W. Weller, C.G. Rader, AIChE J. 21 (1975) 176.
[31] C.G. Rader, S.W. Weller, AIChE J. 20 (1974) 515.
[32] M.E. Garske, M. Harold, Chem. Eng. Sci. 47 (1992) 623.
[33] A.G. Mayer, Papers from the Marine Biological Laboratories at Tortugas, vol. 6, 1914, p. 25.
[34] M.D. Graham, S.L. Lane, D. Luss, J. Phys. Chem. 97 (1993) 7564.
[35] S.Y. Yamamoto, C.M. Surko, M.B. Maple, R.K. Pina, Phys. Rev. Lett. 74 (1995) 4071.
[36] S.Y. Yamamoto, C.M. Surko, M.B. Maple, R.K. Pina, J. Chem. Phys. 102 (1995) 8614.
[37] M.A. Liauw, M. Somani, J. Annamalai, D. Luss, AIChE J. 43 (1997) 1519.
[38] J. Annamalai, C. Ballandis, M. Somani, M.A. Liauw, D. Luss, J. Chem. Phys. 107 (1997) 1896.
[39] M.D. Graham, M. Bär, I.D. Keverikidis, K. Askura, J. Lauterbach, K. Krischer, H.H. Rotermund, G. Ertl, Phys. Rev. E 52 (1995) 76.
[40] M.D. Graham, I.D. Keverikidis, K. Askura, J. Lauterbach, K. Krischer, H.H. Rotermund, G. Ertl, Science 82 (1994) 264.
[41] A.K. Bangia, M. Baer, I.G. Kevrekidis, M.D. Graham, H.-H. Rotermund, G. Ertl, Chem. Eng. Sci. 51 (1966) 1757.
[42] J. Christoph, R.D. Otterstedt, M. Eiswirth, N.I. Jaeger, J.L. Hudson, Phys. Rev. E 58 (1998) 6810.
[43] R.D. Otterstedt, N.I. Jaeger, P.J. Plath, J. Hudson, Chem. Eng. Sci. 54 (1999) 1221.
[44] J. Lee, J. Christoph, P. Strasser, M. Eiswirth, G. Ertl, Phys. Chem. Chem. Phys. 5 (2003) 935.
[45] A. Birzu, F. Plenge, N.I. Jaeger, J.L. Hudson, K. Krischer, J. Chem. Phys. Chem. 110 (2003) 8614.
[46] F. Plenge, Y.Y. Li, K. Kricher, J. Phys. Chem. 108 (2004) 14255.
[47] B.Y. Kogan, W.I. Karplus, B.S. Billett, W.G. Stevenson, Physica D 59 (1992) 349.
[48] J.M. Davidenko, A.v. Petrosov, R. Salomonsz, W. Baxter, J. Jalife, Nat. (Lond.) 355 (1992) 349.
[49] Z. Qu, J.N. Weiss, A. Garfinkel, Phys. Rev. Lett. 78 (1997) 1387.
[50] R.A. Schmitz, T.T. Tsosis, Chem. Eng. Sci. 38 (1983) 1431.
[51] M. Golubitsky, I. Stewart, in: P. Holmes, P. Newton, A. Weinstein (Eds.), Geometry, Dynamics, and Mechanics, Springer-Verlag, Berlin, 2002, p. 243.
[52] M. Golubitsky, M. Nicol, I. Stewart, J. Nonlinear Sci. 14 (2) (2004) 119.
[53] P.K. Tsai, M.B. Maple, R.K. Herz, J. Catal. 113 (1988) 453.
[54] E. Wicke, H.U. Onken, Chem. Eng. Sci. 43 (1988) 2289.
[55] E. Wicke, H.U. Onken, in: M. Markus, S.C. Muller, G. Nicolis (Eds.), From Chemical to Biological Organization, Springer-Verlag, Berlin, 1988, p. 68.
[56] J.L. Gland, G.B. Fisher, E.B. Kollin, J. Catal. 72 (1982) 263.
[57] D. Bocker, E. Wicke, in: L. Rensing, N.I. Jaeger (Eds.), Temporal Order, vol. 75, Springer, Berlin, 1984.
[58] R.M. Ziff, E. Gulari, Y. Brashad, Phys. Rev. Lett. 56 (1986) 2553.
[59] O. Lev, M. Sheintuch, L.M. Pismen, H. Yarnitski, Nature 338 (1988) 458.
[60] U. Middya, D. Luss, M. Sheintuch, J. Chem. Phys. 100 (1994) 3568.
[61] U. Middya, M.D. Graham, D. Luss, M. Sheintuch, J. Chem. Phys. 98 (1993) 2823.
[62] M. Somani, M.A. Liauw, D. Luss, Chem. Eng. Sci. 52 (1997) 2331.
[63] M. Somani, M. Liauw, D. Luss, Chem. Eng. Sci. 51 (1996) 4259.
[64] J. Annamalai, M. Liauw, D. Luss, Chaos 9 (1999) 36.
[65] J.R. Brown, G.A. D'netto, R.A. Schmitz, in: L. Rensig, N. Jaeger (Eds.), Temporal Order, Springer Verlag, Berlin, 1986, p. 86.
[66] J.C. Kellow, E.E. Wolf, Chem. Eng. Sci. 45 (1990) 2597.
[67] J.C. Kellow, E.E. Wolf, AIChE J. 37 (1991) 1844.
[68] F. Qin, E.E. Wolf, Ind. Eng. Chem. Res. 34 (1995) 2923.
[69] J. Puszynnski, V. Hlavacek, Chem. Eng. Sci. 39 (1984) 681.
[70] A.B. Rovinski, M. Menzinger, Phys. Rev. Lett. 70 (1993) 78.
[71] Y.S. Matros, Unsteady Processes in Catalytic Reactors, Elsevier, Amsterdam, 1985.
[72] B. Marwaha, D. Luss, AIChE J. 48 (2002) 617.
[73] B. Marwaha, D. Luss, Chem. Eng. Sci. 58 (2003) 733.
[74] B.B. Marwaha, S. Sundarram, D. Luss, J. Phys. Chem. 108 (2004) 14470.
[75] B. Marwaha, S. Sundarram, D. Luss, Chem. Eng. Sci. 59 (2004) 5569.
[76] R. Digilov, O. Nekhamkina, M. Sheituch, AIChE J. 50 (2004) 163.
[77] V.D. Belyaev, M.M. Slinko, V.I. Timoshenko, M.G. Slinko, Kinet. Catal. 14 (1973) 810.
[78] M. Sheintuch, O. Nekhamkina, Catal. Today 70 (2001) 369.
[79] M. Sheintuch, R.A. Schmitz, Catal. Rev. Sci. Eng. 15 (1977) 107.

[80] D.J. Kaul, R. Sant, E.E. Wolf, Chem. Eng. Sci. 42 (1987) 1399.
[81] M. Sheintuch, Physica D 102 (1997) 125.
[82] J.E. Turner, B.C. Sales, M.B. Maple, Surf. Sci. 103 (1981) 54.
[83] M.M. Slinko, E.S. Kurkina, M.A. Liauw, N.I. Jaeger, J. Chem. Phys. 111 (1999) 8105.
[84] O. Nekhamkina, M. Sheintuch, J. Chem. Phys., in press.
[85] U. Middya, M. Sheintuch, M.D. Graham, D. Luss, Physica D 63 (1993) 393.
[86] O. Nekhamkina, M. Sheintuch, J. Chem. Phys. 122 (2005) 194701.
[87] M. Sheintuch, Chem. Eng. Sci. 44 (1989) 1081.
[88] U. Middya, D. Luss, J. Chem. Phys. 102 (1995) 5029.
[89] M. Sheintuch, O. Nekhamkin, J. Chem. Phys. 107 (1997) 8165.
[90] I. Savin, O. Nekhamkina, M. Sheintuch, J. Chem. Phys. 115 (2001) 7678.
[91] O. Nekhamkina, R.M. Digilov, M. Sheintuch, J. Chem. Phys. 119 (2003) 2322.
[92] M. Sheintuch, O. Nekhamkina, J. Chem. Phys. 109 (1998) 10612.
[93] M. Sheintuch, J. Chem. Phys. 105 (1996) 289–298.
[94] D.A. Frank-Kamenetski, Diffusion and Heat Transfer in Chemical Kinetics, second ed., Plenum Press, NY, 1969.
[95] E. Wicke, D. Vortmeyer, Z. Elektochem. Ber. Bunsenges. Phys. Chem. 63 (1959) 145.
[96] V. Pinjala, Y.C. Chen, D. Luss, AIChE J. 34 (1988) 1663.
[97] K.F. Jensen, H.W. Ray, Chem. Eng. Sci. 37 (1982) 199.
[98] V. Balakotayah, E.L. Christoforatou, D.H. West, Chem. Eng. Sci. 54 (1999) 1725.
[99] Y.Z. Yakhnin, M. Menzinger, Chem. Eng. Sci. 56 (2001) 2233.
[100] Y.Sh. Matros, G.A. Bunimovich, Catal. Rev. Sci. Eng. 38 (1996) 1.
[101] G. Kolios, J. Frauhammer, G. Eigenberger, Chem. Eng. Sci. 55 (2000) 5459.
[102] M. Ben-Tullilah, E. Alajem, R. Gal, M. Sheintuch, AIChE J. 49 (2003) 1849.
[103] G. Lauschke, E.D. Gilles, Chem. Eng. Sci. 49 (1994) 5359.
[104] O. Nekhamkina, M. Sheintuch, AIChE J. 51 (2004) 224.
[105] M. Brinkmann, A.A. Barresi, M. Vanni, G. Baldi, Catal. Today 47 (1999) 263.
[106] M. Sheintuch, O. Nekhamkina, AIChE J. 45 (1999) 398.
[107] M. Sheintuch, O. Nekhamkina, Chem. Eng. Sci. 54 (1999) 4535.
[108] M. Barto, M. Sheintuch, AIChE J. 40 (1994) 120.
[109] D. Vortmeyer, R.J. Schaefer, Chem. Eng. Sci. 29 (1974) 485.
[110] I. Keren, M. Sheintuch, Chem. Eng. Sci. 55 (2000) 1461.
[111] D.T. Leighton, H.C. Chang, AIChE J. 41 (1995) 1898.
[112] G. Viswanathan, A. Bindal, J. Khinast, D. Luss, AIChE J., in press.
[113] M. Sheintuch, O. Nekhamkina, Chem. Eng. Sci. 58 (2003) 1441.
[114] O. Nekhamkina, I. Savin, M. Sheintuch, J. Chem. Phys. 117 (2002) 7329.
[115] K. Kladko, I. Mitkov, A.R. Bishop, Phys. Rev. Lett. 84 (2000) 4505.
[116] M. Morbidelli, A. Varma, R. Aris, in: J.J. Carberry, A. Varma (Eds.), Chemical Reaction and Reactor Engineering, Marcel Dekker, 1986.
[117] A.N.R. Bos, L. Vandebeld, J.B. Overkamp, K.R. Westerterp, Chem. Eng. Commun. 121 (1993) 27.
[118] J.C. Comte, S. Morfu, P. Marquié, Phys. Rev. E 64 (2001) 027102.
[119] Y. Kuramoto, Chemical Oscillations, Waves and Turbulence, Springer, Berlin, 1984.
[120] I.Z. Kis, Y. Zhai, J.L. Hudson, Science 296 (2002) 1676.
[121] S. De Monte, F. d'Ovidio, E. Mosekilde, Phys. Rev. Lett. 90 (2003) 054102.
[122] Y.C. Chen, D. Luss, AIChE J. 35 (1989) 1148.
[123] S.M.S. Dommeti, V. Balakotaiah, D. West, Ind. Eng. Chem. Res. 38 (1999) 767.
[124] V. Balakotaiah, S.M.S. Dommeti, Chem. Eng. Sci. 54 (1999) 1621.
[125] F. Stroh, V. Balakotaiah, AIChE J. 37 (1991) 1035.
[126] D. Nguyen, V. Balakotaiah, Proc. R. Soc. Lond. A 450 (1995) 1–21.
[127] J.E. Gatica, H.J. Viljoen, V. Hlavacek, Chem. Eng. Sci. 44 (1989) 1853.
[128] N.V. Peskov, M.M. Slinko, N.I. Jaeger, J. Chem. Phys. 118 (2003) 8882.